A11102 154538
NAT'L INST OF STANDARDS & TECH R.I.C.
A11102154538
/NBS building science series
TA435 .U58 V151;1983 C.2 NBS-PUB-C 1974

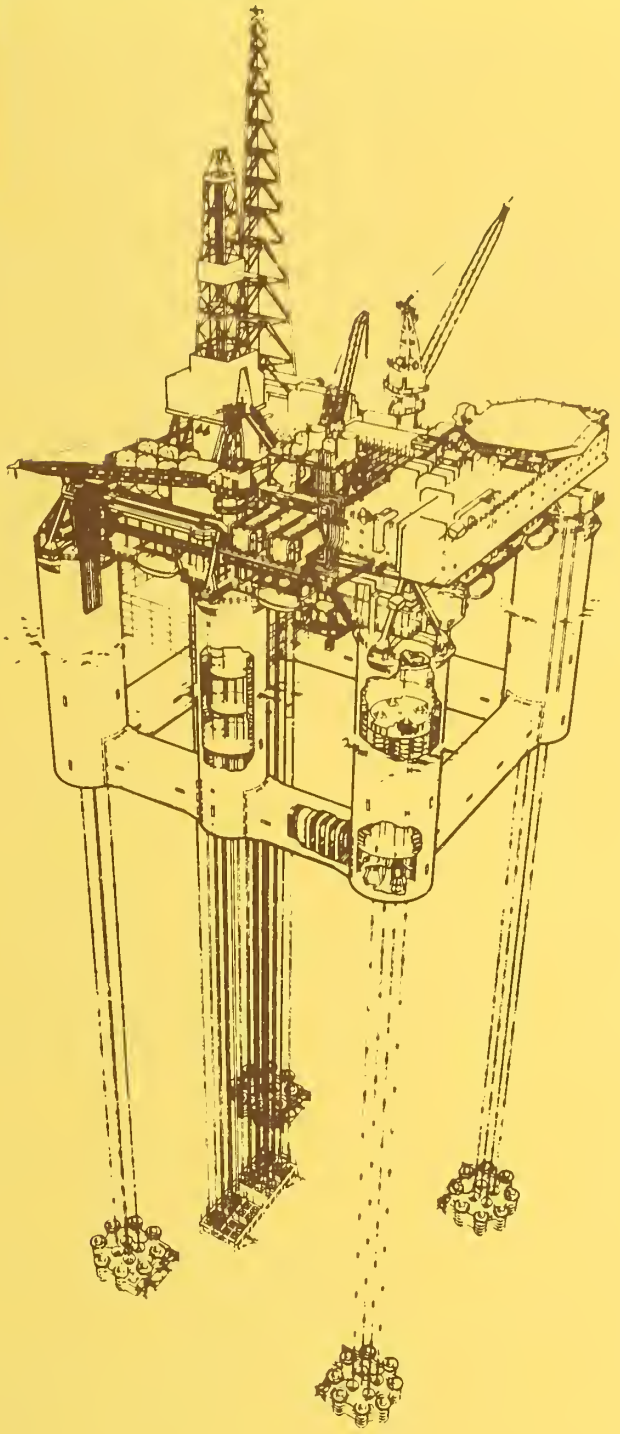

TA
435
.U58
151
1983
C.2

NBS BUILDING SCIENCE SERIES 151

Turbulent Wind Effects on Tension Leg Platform Surge

U.S. DEPARTMENT OF COMMERCE • NATIONAL BUREAU OF STANDARDS

NATIONAL BUREAU OF STANDARDS

The National Bureau of Standards[1] was established by an act of Congress on March 3, 1901. The Bureau's overall goal is to strengthen and advance the Nation's science and technology and facilitate their effective application for public benefit. To this end, the Bureau conducts research and provides: (1) a basis for the Nation's physical measurement system, (2) scientific and technological services for industry and government, (3) a technical basis for equity in trade, and (4) technical services to promote public safety. The Bureau's technical work is performed by the National Measurement Laboratory, the National Engineering Laboratory, and the Institute for Computer Sciences and Technology.

THE NATIONAL MEASUREMENT LABORATORY provides the national system of physical and chemical and materials measurement; coordinates the system with measurement systems of other nations and furnishes essential services leading to accurate and uniform physical and chemical measurement throughout the Nation's scientific community, industry, and commerce; conducts materials research leading to improved methods of measurement, standards, and data on the properties of materials needed by industry, commerce, educational institutions, and Government; provides advisory and research services to other Government agencies; develops, produces, and distributes Standard Reference Materials; and provides calibration services. The Laboratory consists of the following centers:

Absolute Physical Quantities[2] — Radiation Research — Chemical Physics — Analytical Chemistry — Materials Science

THE NATIONAL ENGINEERING LABORATORY provides technology and technical services to the public and private sectors to address national needs and to solve national problems; conducts research in engineering and applied science in support of these efforts; builds and maintains competence in the necessary disciplines required to carry out this research and technical service; develops engineering data and measurement capabilities; provides engineering measurement traceability services; develops test methods and proposes engineering standards and code changes; develops and proposes new engineering practices; and develops and improves mechanisms to transfer results of its research to the ultimate user. The Laboratory consists of the following centers:

Applied Mathematics — Electronics and Electrical Engineering[2] — Manufacturing Engineering — Building Technology — Fire Research — Chemical Engineering[2]

THE INSTITUTE FOR COMPUTER SCIENCES AND TECHNOLOGY conducts research and provides scientific and technical services to aid Federal agencies in the selection, acquisition, application, and use of computer technology to improve effectiveness and economy in Government operations in accordance with Public Law 89-306 (40 U.S.C. 759), relevant Executive Orders, and other directives; carries out this mission by managing the Federal Information Processing Standards Program, developing Federal ADP standards guidelines, and managing Federal participation in ADP voluntary standardization activities; provides scientific and technological advisory services and assistance to Federal agencies; and provides the technical foundation for computer-related policies of the Federal Government. The Institute consists of the following centers:

Programming Science and Technology — Computer Systems Engineering.

[1]Headquarters and Laboratories at Gaithersburg, MD, unless otherwise noted; mailing address Washington, DC 20234.
[2]Some divisions within the center are located at Boulder, CO 80303.

MAY 17 1983

NBS BUILDING SCIENCE SERIES 151

Turbulent Wind Effects on Tension Leg Platform Surge

Emil Simiu

Center for Building Technology
National Engineering Laboratory
National Bureau of Standards
Washington, DC 20234

and

Stefan D. Leigh

Center for Applied Mathematics
National Engineering Laboratory
National Bureau of Standards
Washington, DC 20234

Sponsored by:

Minerals Management Service
United States Department of the Interior
Reston, VA 22091

U.S. DEPARTMENT OF COMMERCE, Malcolm Baldrige, Secretary
NATIONAL BUREAU OF STANDARDS, Ernest Ambler, Director

Issued March 1983

Library of Congress Catalog Card Number: 83-600507

National Bureau of Standards Building Science Series 151
Natl. Bur. Stand. (U.S.), Bldg. Sci. Ser. 151, 46 pages (Mar. 1983)
CODEN: BSSNBV

U.S. GOVERNMENT PRINTING OFFICE
WASHINGTON: 1983

For sale by the Superintendent of Documents, U.S. Government Printing Office, Washington, D.C. 20402
Price $4.75
(Add 25 percent for other than U.S. mailing)

ABSTRACT

A procedure is presented for estimating surge response to turbulent wind in the presence of current and waves. The procedure accounts for the nonlinearity of the hydrodynamic forces with respect to surge and for the coupling of aerodynamic and hydrodynamic effects. It is shown that current wind spectra do not model correctly the wind speed fluctuations at very low frequencies and an alternative model of the wind spectrum, consistent with fundamental principles, is presented. The equation of surge motion under turbulent wind in the presence of current and waves is solved for typical tension leg platforms, and it is shown that under extreme wave conditions the damping provided by the hydrodynamic forces precludes the occurrence of significant wind-induced resonant amplification effects even if the drag coefficient in the Morison equation is very small (e.g., $C_d = 0.1$). It is verified that for the platforms being investigated the use of a one-minute wind speed to represent the effect of the mean wind and of the turbulent wind fluctuations is acceptable for the purpose of estimating peak surge response.

Key Words: compliant platforms; ocean engineering; offshore platforms; structural engineering; tension leg platforms; turbulence; waves; wind loads.

ACKNOWLEDGMENTS

The cover picture is excerpted from "Hutton TLP Vessel - Structural Configuration and Design Features" by Norman Ellis and Jeffery Howard Tetlow of Conoco (U.K.) Ltd., Fraser Anderson of Scott Lithgow Ltd., and Alan Lindsay Woodhead of Brown and Root (U.K.) Ltd., paper OTC 4427, Proceedings, 1982 Offshore Technology Conference, May 3-6, 1982, Houston, TX, Vol. 4, pp. 557-571.

The writers would like to acknowledge the use of documentation on tension leg platform designs kindly provided by Mr. G. Sebastiani, Manager, Research Department, Tecnomare S.p.A., Venice, Italy.

The writers would also like to express their apppreciation to Ms. Mary Ramsburg for her capable typing effort, and to Ms. Jennie Covahey for her editorial assistance.

TABLE OF CONTENTS

	Page
ABSTRACT	iii
ACKNOWLEDGMENTS	iv
LIST OF SYMBOLS	vi
LIST OF FIGURES	x
LIST OF TABLES	xi
1. INTRODUCTION	1
2. WIND LOADS	3
2.1 Basic Expressions	3
2.2 Mean Wind Speeds	3
2.3 Fluctuating Wind Speeds: Critique of NBC Spectrum	4
2.4 Fluctuating Wind Speeds: Proposed Spectrum	6
2.5 Fluctuating Wind Speeds: Spatial Coherence	6
2.6 Mean Wind Loads	10
2.7 Fluctuating Wind Loads	10
3. Hydrodynamic Loads	15
4. Restoring Force	17
5. Numerical Estimates	19
5.1 Equation of Surge Motion	19
5.2 Assumed Characteristics of Environment and of Platforms	19
5.3 Linear vs. Nonlinear Restoring Force	21
5.4 Nominal Damping Ratio of Pseudo-Linear System Equivalent to Equation 38	24
5.5 Peak Surge Response Under Turbulent Winds	27
5.6 Surge Response Estimated Under Various Simplifying Assumptions	27
5.7 Sensitivity of Surge Response to Changes in Values of Wind Environment and Aerodynamic Parameters	30
6. SUMMARY AND CONCLUSIONS	33
REFERENCES	35
APPENDIX - Expression for the Spectrum of the Longitudinal Velocity Fluctuations	39

LIST OF SYMBOLS

A = surge added mass

A_a = projection of above-water part of platform on plane normal to wind speed

$A_{p_{ij}}$ = elemental area of submerged structure projected on a plane normal to direction of current and wave motion

b = width of main deck

B = surge wave-radiation damping coefficient

C_a = overall aerodynamic drag coefficient defined by Eq. 17

C_c, C_m = drag inertia coefficient in Morison's equation, respectively

C_{Dsea} = sea drag coefficient (Eq. 5)

$C_{d_{ij}}, C_{m_{ij}}$ = drag, inertia coefficient in Morison's equation corresponding to volume $\forall_{ij}$, respectively

C_{NL} = downdraw coefficient (Eq. 37)

Coh = square root of coherence function (Eq. 15)

C_p = pressure coefficient (Eq. 1)

C_y, C_z = exponential decay coefficients (Eq. 16)

D, D_c = diameter of immersed body or component, diameter of buoyant columns, respectively

E = function defined by Eq. 29

f, f_m, f_s = nondimensional frequency, nondimensional frequency at which product nS_u is maximum, nondimensional frequency above which Eq. A1c is valid

F_h, F_e, $F'_{equ,r}$, F_u, $F'_{u,r}$, F_v = total hydrodynamic load, total wave-induced exciting force, equivalent force defined by Eq. 23, total wind load, fluctuating part of wind load acting on body at rest, total hydrodynamic viscous force

g = acceleration of gravity

H = wave height

J = reduction factor defined by Eq. 28

LIST OF SYMBOLS (Continued)

k = von Kármán's constant

k_w = wave number given by Eq. 34

K = Keulegan-Carpenter number

ℓ_n = nominal length of tethers

L = wave length

L_u = integral scale of longitudinal wind velocity fluctuations (in direction of mean wind speed)

M = total mass of platform

M_i = point in space

$\text{Max}(x_{max})$ = sample maximum value of x_{max}

n, n_m = frequency

p = wind pressure

R = restoring force

Re = Reynolds number

R_u = autocovariance function of longitudinal velocity fluctuations

$s(x_{max})$ = sample standard deviation of x_{max}

$S_{F_{equ,r}}, S_{F_{u,r}}$ = spectrum of $F'_{equ,r}$, of $F'_{u,r}$, respectively

$S_u, S_{u_1u_2}, S^C_{u_1u_2}$ = spectrum, cross-spectrum, cospectrum of longitudinal velocity fluctuations, respectively

S_{ueq} = spectrum of equivalent wind speed fluctuations, defined by Eq. 21

t = time

T = total tension in tethers at $x = 0$

T_f = period of harmonic relative fluid-body motion

T_n = nominal natural period of surge motion

T_w = wave period

u, u', u'_{eq}, u'_{eqj} = longitudinal wind velocity, longitudinal velocity fluctuation, equivalent wind speed fluctuation, component of equivalent wind speed fluctuation

u_* = friction velocity

$\overline{v_i}$ = current velocity

v_{ij} = horizontal wave-induced velocity at coordinates z_i, X_j

$\overline{V}$ = amplitude of relative fluid-body velocity

$\forall_{ij}$ = elemental submerged volume

x = platform surge displacement

x_{max} = peak surge displacement

x_{umax} = amplitude of contribution to surge of a harmonic force (Eq. 14)

X = horizontal coordinate

y, y_i = horizontal coordinate, horizontal coordinate of point M_i, respectively

Y_i = arbitrary coordinate

z = vertical coordinate above mean water level

z_{ij} = vertical distance from free surface to center of volume $\forall_{ij}$

z_o = roughness length

β = coefficient defining mean square value of turbulent fluctuation in terms of friction velocity (Eq. 14)

Δ = denotes increment of a quantity

ζ = nominal damping ratio

ν = dynamic viscosity

ρ_a, ρ_w = air, water density, respectively

τ = time lag

ϕ = arbitrary function

ϕ_j = phase angle

$\dot{}$ = denotes differentiation with respect to time

$\bar{}$ = denotes mean value

$'$ = denotes fluctuating part

LIST OF FIGURES

		Page
Figure 1.	Spectra of Longitudinal Velocity Fluctuations	7
Figure 2.	Spectra of Longitudinal Velocity Fluctuations	8
Figure 3.	Spectra of Longitudinal Velocity Fluctuations	9
Figure 4.	Integration Domain and Transformation of Variables	12
Figure 5.	Geometry of Tension Leg Platform	20
Figure 6.	Surge Response of Tension Leg Platform with Nonlinear Restoring Force	22
Figure 7.	Surge Response of Tension Leg Platform with Linear Restoring Force	23
Figure 8.	Surge Response of Tension Leg Platform to Harmonic Wind Load in the Presence of Current and Waves, $C_m = 1.8$, $C_d = 0.8$	26
Figure 9.	Surge Response of Tension Leg Platform to Turbulent Wind Load in the Presence of Current and Waves	28

LIST OF TABLES

		Page
Table 1.	Assumed Current Speeds at Various Depths z_i	19
Table 2.	Estimated Nominal Damping Ratio, ζ, and Mean and Peak Surge Response $\bar{x}$ and x_{pk}, in Meters	25
Table 3.	Statistics of Peak Surge Response, x_{max}, Under Turbulent Winds (in meters)	27
Table 4.	Estimates of Surge Response Corresponding to Various Deterministic Loading Assumptions (in meters)	29
Table 5.	Dependence of $J^{1/2}(n)$ Upon Exponential Decay Coefficient, C_y ..	31
Table 6.	Dependence of $\overline{u(z)}$ Upon z_o ($\overline{u(35\ m)}$ = 45 m/s)	31

1. INTRODUCTION

Wind effects on tension leg platform (TLP) surge response can be divided into two categories: the wind-induced steady drift, due in practice solely to the mean wind speed, and oscillatory motions induced by the turbulent wind speed fluctuations.

If the requisite aerodynamic information is available the estimation of the wind-induced steady drift is straightforward. However, the estimation of the wind-induced oscillation raises a number of problems that merit careful investigation. It has been stated [24] that "determining the response to wind is possibly of greater importance to the design of compliant structures than the wave and current aspects. Wind has a spectrum which has its peak near the structure's natural frequency in surge. In many instances, the movements derived from varying wind will be greater than those for the wave drift."

Investigations into wind-induced oscillatory compliant platform motions have been reported recently in references 6 and 28. However, these investigations do not take into account nonlinearities due to the hydrodynamic viscous forces, and assume instead that the response to wind is described by a system with proportional damping, the damping ratio being of the order of 5 percent. It appears that no research has been reported that takes into account explicitly the turbulent nature of wind as reflected by spectral and cross-spectral information, while considering simultaneously the nonlinear effects of current and waves. Rather, estimates of the effect of wind speed fluctuations in the presence of current and waves have been advanced that assume a constant (1-minute wind) or harmonic loading in lieu of the actual turbulent wind load [11, 17, 19]. The extent to which these simplified representations are acceptable has not yet been established in the literature. This was noted in a recent evaluation of the Hutton TLP response to environmental loads, which states: "Wind gusts are typically broad-banded and may contain energy which could excite surge motions at the natural period. These would be controlled by surge damping. Theoretical and experimental research is required to clarify the importance of this matter" [11]. The investigation presented here was undertaken in response to this need.

In this paper the surge response is estimated by solving the equation of surge motion in the time domain. The forces represented in this equation consist of: the forces of inertia, the external forces (hydrodynamic and aerodynamic), and the internal forces (restoring, and damping due to internal friction within the structure).

In the following sections the models used in this investigation for the external and internal forces are described, and the equation of surge motion is solved for TLP's with specified characteristics in specified wave, current, and wind environments. To gain insights into the behavior of the platform viewed as a hydrodynamically damped system, the equation of surge motion is also solved in the idealized case where the fluctuating wind load is represented by a harmonic function. Numerical results are presented, and their sensitivity to changes in the values of various parameters is assessed. Current simplified wind loading models are evaluated in light of these results.

2. WIND LOADS

2.1 BASIC EXPRESSIONS

Like the hydrodynamic loads, the wind loads consist of a component due to the presence of viscosity and the consequent flow separation, and an inertial component associated with the relative fluid-body accelerations. However, it can be verified that the inertial component is about two orders of magnitude smaller than the component due to flow separation, and can therefore be neglected in practical applications.

To estimate the wind-induced drag force it is assumed that the elemental drag force per unit of area projected on a plane, P, normal to the mean wind speed can be written as:

$$p(y,z,t) = \frac{1}{2} \rho_a \, C_p(y,z)[u(y,z,t) - \dot{x}(t)]^2 \tag{1}$$

where ρ_a = air density, $C_p(y,z)$ = pressure coefficient at elevation z and horizontal coordinate y in the plane P, t = time, x = surge displacement, the dot denotes differentiation with respect to time, and u(y,z,t) = wind speed upwind of the structure in the direction of the mean wind. It is assumed that the directions of the mean wind and of the surge motion coincide. The speed, u(y,z,t), can be expressed as:

$$u(y,z,t) = \overline{u(z)} + u'(y,z,t) \tag{2}$$

where the bar and the prime indicate mean value and fluctuating part, respectively. The total wind-induced drag force is

$$F_u(t) = \int_{A_a} p(y,z,t) \, dy \, dz \tag{3}$$

where A_a = projection of above-water part of the platform on a plane normal to the mean wind speed.

It is seen that a prerequisite for the modeling of the elemental and total drag forces is the modeling of the wind speed, u(y,z,t).

2.2 MEAN WIND SPEEDS

The mean wind speed can be modeled by the equation:

$$\overline{u(z)} = \overline{u(z_{ref})} \, \frac{\ell n \, \frac{z}{z_o}}{\ell n \, \frac{z_{ref}}{z_o}} \tag{4}$$

where z_{ref} = reference elevation (usually in meteorological practice z_{ref} = 10 m), and z_o = roughness length.

Information on the roughness length, z_o, over the ocean is commonly provided by specifying the value of the sea drag coefficient, defined as

$$C_{Dsea} = [k/\ell n(10/z_o)]^2 \tag{5}$$

where z_o is expressed in meters and k = von Kármán constant ($k \simeq 0.4$). Measurements have shown that the sea drag coefficient increases with wind speed. This dependence is not completely understood; however, on the basis of a large number of measurements, the following empirical relations were proposed for the range $4 < \overline{u}(10) < 21$ m/s:

$$C_{Dsea} = 5.1 \times 10^{-4} \, [\overline{u(10)}]^{0.46} \tag{6}$$

or

$$C_{Dsea} = 10^{-4} \, [7.5 + 0.67 \, \overline{u(10)}] \tag{7}$$

where $\overline{u}(10)$ is expressed in m/s [25]. For values of about $\overline{u}(10) > 20$ m/s the variation of C_{Dsea} with wind speed appears to be insufficiently documented. According to reference 29, for such values C_{Dsea} is constant. On the other hand, results of limited studies summarized in reference 5 would suggest that for about $\overline{u}(10) > 20$ m/s C_{Dsea} can be expressed as an average of the values given by equations 6 and 7.

It is shown subsequently that uncertainties with respect to the actual value of C_{Dsea} are of little consequence in the estimation of the total surge response; errors in the estimation of C_{Dsea} of the order of 50 percent result in differences in the calculated total surge of less than 5 percent. Note that, even if the actual value of z_o were known, equation 4 should not be regarded as "exact," particularly near the mean water surface. Indeed, it is argued in reference 9 that owing to the presence of waves "wind profiles are distorted to lower wind speeds compared to flow above a rigid surface." The use of equation 4 in structural calculations is therefore likely to be conservative.

2.3 FLUCTUATING WIND SPEEDS: CRITIQUE OF NBC SPECTRUM

For design purposes, it is necessary to describe the longitudinal wind speed fluctuations, u', in equation 2 in terms of their spectra and cospectra [23, p. 446].

The expression for the spectrum of the longitudinal velocity fluctuations used in the National Building Code of Canada (NBC) [12] and the American National Standard ANSI A58.1 - 1972 [1] is

$$S_u^{NBC}(n) = 4u_*^2 \frac{[1{,}200/\overline{u(10)}]^2 n}{\{1+[1200n/\overline{u(10)}]^2\}^{4/3}} \tag{8}$$

where n = frequency, $\overline{u}(10)$ is expressed in m/s, and the friction velocity, u_* is defined as

$$u_* = \frac{k\ \overline{u(10)}}{\ell n\ \frac{10}{z_o}} \tag{9}$$

Equation 8 is represented in figure 1 for u_* = 1.76 m/s and C_{Dsea} = 0.002 (z_o = 0.0013 m). It is seen that according to equation 8 the ordinates of the spectrum at frequencies of interest in deep water platform design (i.e., n ≃ 0.01 Hz) are quite small. However, this is actually not the case. As pointed out by Lumley and Panofsky [10], the assumption inherent in equation 8 to the effect that the spectrum vanishes at n = 0 is incorrect. This can be shown by considering the relationship between the spectrum and the autocovariance function, $R_u(\tau)$:

$$S_u(n) = 4 \int_0^\infty R_u(\tau) \cos 2\pi n\tau d\tau \tag{10}$$

For n = 0:

$$S_u(0) = 4 \int_0^\infty R_u(\tau)\, d\tau \tag{11}$$

The function $R_u(\tau)$ decreases with increasing τ from $R_u(0) = \overline{u'^2}$ to $R_u(\tau) \simeq 0$ for large values of τ. Defining the integral length scale of the longitudinal turbulence as

$$L_u = \frac{\overline{u}}{\overline{u'^2}} \int_0^\infty R_u(\tau)\, d\tau \tag{12}$$

it follows immediately from equations 11 and 12 that

$$S_u(0) = 4 \frac{\overline{u'^2}}{\overline{u}} L_u \tag{13}$$

Information on L_u and its variation in the atmosphere cannot be obtained from wind tunnel measurements, owing to the difficulty of modeling the mesometeorological features that presumably control the lower frequency portions of the spectra [13]. However, values of L_u obtained from numerous full-scale measurements are listed in the literature, and in particular in reference 2. These show that L_u increases with height above ground, and that it also increases if the surface roughness decreases. From these measurements it may be inferred roughly that at elevations over water of about 20 to 60 m, which are of primary interest in platform design, 100 m < L_u < 240 m. Even larger variations (60 m < L_u < 450 m) were reported by Shiotani [22] (see also reference 23, p. 55). The effect of such variations upon the magnitude of surge response is examined subsequently.

2.4 FLUCTUATING WIND SPEEDS: PROPOSED SPECTRUM

No expression for the wind spectrum compatible with equation 13 has been developed so far in the literature primarily because the shape of the spectrum in the very low frequency range has little effect on the design of land-based structures or fixed offshore platforms [23]. To develop such an expression the following conditions, in addition to equation 13, must be satisfied (for details, see reference 23, pp. 53-55):

1. In the inertial subrange ($f > f_s$), where the nondimensional frequency $f = nz/\overline{u(z)}$, and $f_s \simeq 0.2$, Kolmogorov's first and second hypothesis apply, and the energy production is approximately balanced by the energy dissipation.

2. The product $nS_u(n)$ is a maximum (i.e., the derivative of the function $nS_u(n)$ vanishes) at some nondimensional frequency, $f_m < f_s$. Measurements at elevations of interest in platform design suggest that $f_m \simeq 0.05$ to 0.09.

3. The area under the spectral curve is

$$\overline{u'^2} \simeq \beta u_*^2 \tag{14}$$

where u_* is defined by equation 9 and $\beta \simeq 6.0$.

An expression for the spectrum derived from these conditions and Eq. 13 is given in the appendix (equation A1). This expression is plotted in figure 1 for $k = 0.4$, $z_o = 0.001266$ m, $z = 35$ m, $\overline{u(35)} = 45$ m/s ($u_* = 1.76$ m/s), $\beta = 6.0$, $f_s = 0.2$, $f_m = 0.07$, and $L_u = 180$ m. For the same values of the parameters k through f_s, the expression for the spectrum is also plotted in figure 2 for $f_m = 0.07$ and $L_u = 100$ m, 180 m, and 240 m, and in figure 3 for $L_u = 180$ m and $f_m = 0.05$, 0.07, and 0.09. It is seen from figure 3 that the influence of the nondimensional frequency f_m on the shape of the spectrum is weak.

2.5 FLUCTUATING WIND SPEEDS: SPATIAL COHERENCE

It is a characteristic of turbulent flows that the velocity fluctuations at any two points separated by some distance, d, do not exhibit perfect mutual coherence. Owing to imperfect coherence such fluctuations do not attain their maxima or minima at the same time, and the resultant wind-induced fluctuating loads are lower than would be the case if perfect spatial coherence were assumed. Mathematically, the imperfect coherence is reflected in the expression for the cross-spectrum of the velocity fluctuations, $S_{u_1u_2}(n)$, whose absolute value can be written as:

$$|S_{u_1u_2}(n)| = S_{u_1}^{1/2}(n)\, S_{u_2}^{1/2}(n)\, \mathrm{Coh}\,(M_1, M_2, n) \tag{15}$$

where $S_{u_1}(n)$ and $S_{u_2}(n)$ = spectra of the velocity fluctuations, u'_1 and u'_2, at points M_1 and M_2, respectively, and Coh (M_1, M_2, n) is referred to as the

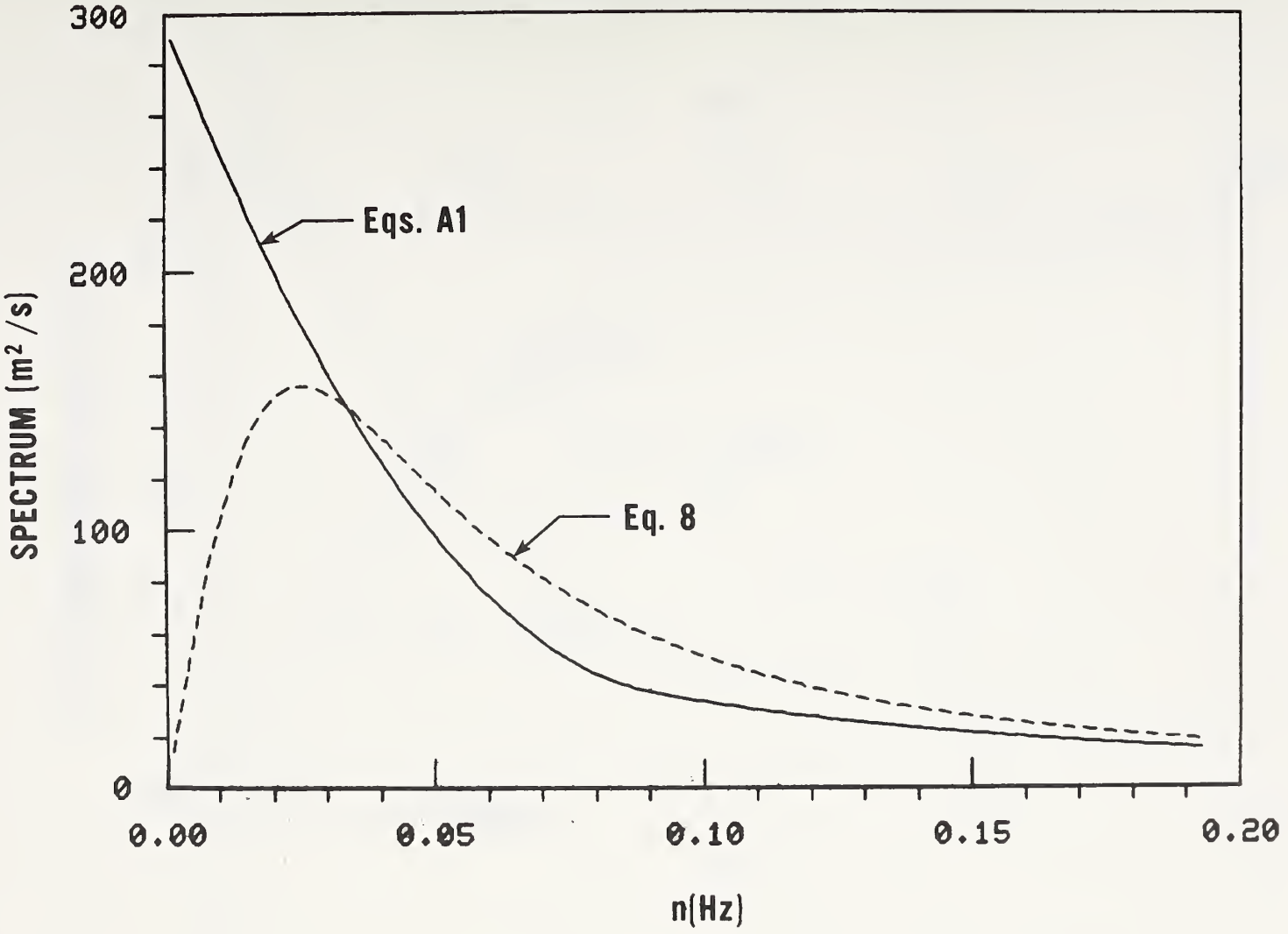

Figure 1. Spectra of longitudinal velocity fluctuations

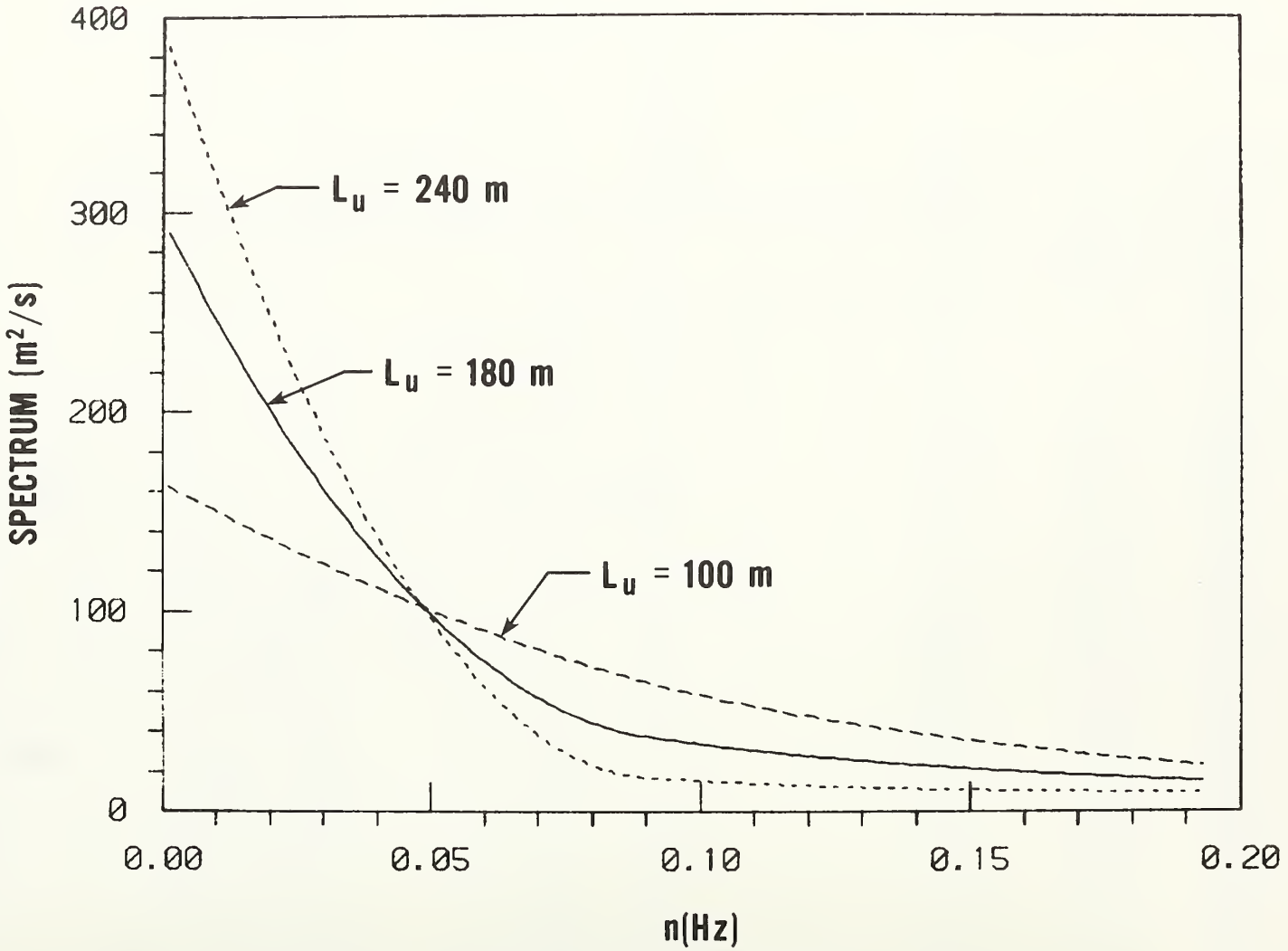

Figure 2. Spectra of longitudinal velocity fluctuations

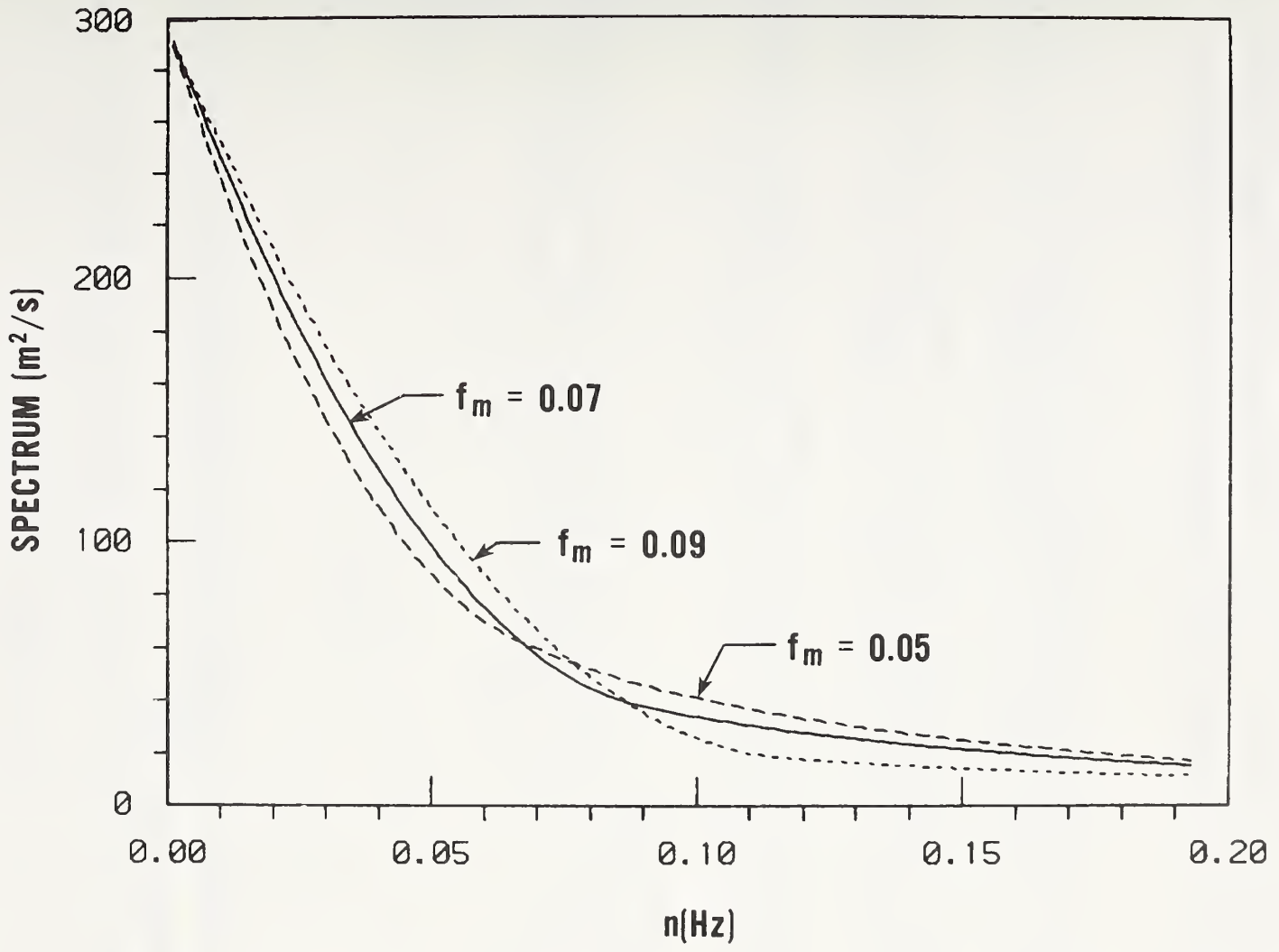

Figure 3. Spectra of longitudinal velocity fluctuations

square root of the coherence function. Coh (M_1, M_2, n) is unity for $M_1 = M_2$ and decreases with increasing distance between M_1 and M_2. For any given M_1 and M_2 the coherence decreases with increasing n. An expression similar to equation 15 can be written for the cospectrum (i.e., the real part of the cross-spectrum) of u_1' and u_2', $S^C_{u_1u_2}(n)$. Measurements have shown that if M_1 and M_2 are contained in a plane normal to the mean velocity, it is possible to write [3]:

$$S^C_{u_1u_2}(n) = S^{1/2}_{u_1}(n)\, S^{1/2}_{u_2}(n) \exp \frac{-[C_y^2(y_1-y_2)^2+C_z^2(z_1-z_2)^2]^{1/2}\, n}{\frac{1}{2}\,[\overline{u(z_1)} + \overline{u(z_2)}]} \tag{16}$$

where C_y, C_z are empirical factors referred to as exponential decay coefficients. Commonly accepted values are $C_y = 10$, $C_z = 16$ [28]. However, actual values as obtained from experiments vary widely [8, 22, 23]. The effect of this variation on the calculated surge response is examined subsequently.

Equation 16 can be modified to include the effect of longitudinal separation (in the direction of the mean wind) as well. However, it follows from information presented in reference 7 that this effect is negligible as far as fluctuating aerodynamic loads on offshore structures are concerned.

2.6 MEAN WIND LOADS

It can be verified that the mean square values of u' and $\dot{x}$ and the mean value of the product $u'\dot{x}$ are small compared to the square of $\bar{u}$. It then follows from equations 1, 2, and 3 that the mean drag load can be written as

$$\overline{F_u(t)} \simeq \frac{1}{2}\,\rho_a\, C_a\, A_a\, \overline{u(z_a)}^2 \tag{17}$$

where the overall aerodynamic drag coefficient is

$$C_a = \frac{1}{A_a\, u(z_a)^2} \int_{A_a} C_p(y,z)\, \overline{u(z)}^2\, dydz \tag{18}$$

and z_a = elevation of aerodynamic center of above-water part of the platform.

2.7 FLUCTUATING WIND LOADS

From equation 1, 2, 3, 17, and 18 it follows that the fluctuating part of the wind drag load that would act on the platform at rest (i.e., with $\dot{x} \equiv 0$) is

$$F'_{u,r}(t) = \rho_a \int_{A_a} C_p(y,z)\, \overline{u(z)}\, u'(z,t)\, dy\, dz \tag{19}$$

where the subscript r refers to the fact that the platform is at rest. The Fourier transform of the autocovariance function of $F'_{u,r}(t)$ yields:

$$S_{F_{u,r}}(n) = \rho_a^2 \int\int_{A_a A_a} C_p(y_1,z_1)\, C_p(y_2,z_2)\, \overline{u(z_1)}\, \overline{u(z_2)}$$

$$C_{u_1 u_2}(y_1,y_2,z_1,z_2)\, dy_1 dy_2 dz_1 dz_2 \qquad (20)$$

where $C_{u_1 u_2}$ is given by equation 16. The spectrum $S_{F_{u,r}}(n)$ can be estimated numerically by assuming $C_p(y_i,z_i) \simeq C_a$ (i=1,2) and using equations 4, 16, and A1 (see appendix). An equivalent wind fluctuation spectrum can then be defined as

$$S_{u,eq}(n) = \frac{S_{F_{u,r}}(n)}{[\rho_a C_a A_a \overline{u(z_a)}]^2} \qquad (21)$$

From $S_{u,eq}(n)$ it is possible to generate by Monte Carlo simulation realizations of the process $u'_{eq}(t)$:

$$u'_{eq}(t) = \sum_j u'_{eqj} \cos(2\pi n_j t + \phi_j) \qquad (22)$$

In equation 22 the phase angle, ϕ_j, is generated by random sampling from a uniform distribution in the interval $0 < \phi_j < 2\pi$.

Let the spectrum of the force, $F'_{equ,r}(t)$, defined as

$$F'_{equ,r}(t) = \rho_a C_a A_a \overline{u(z_a)}\, u'_{eq}(t) \qquad (23)$$

be denoted by $S_{F_{equ,r}}(n)$. Clearly,

$$S_{F_{equ,r}}(n) \simeq S_{F_{u,r}}(n) \qquad (24)$$

Thus, $u'_{eq}(t)$ can be viewed as an equivalent wind speed fluctuation which is perfectly coherent over the area A_a and whose effect upon the structure at rest is the same as that of the actual fluctuating wind field.

The total wind load acting on the platform can thus be expressed as

$$F_u(t) = \frac{1}{2} \rho_a C_a A_a [\overline{u(z_a)} + u'_{eq}(t) - \dot{x}(t)]^2 \qquad (25)$$

Numerical calculations have shown that if the difference between the elevation of the helideck (or the top of the crew quarters) and the underside of the lower deck in a typical drilling and production platform is less than about two-thirds to three quarters of the width of the main deck, the term $C_z^2 (z_1-z_2)^2$ of equation 16 can be neglected when evaluating the integral of equation 20. This is a consequence of the fact that C_z is smaller than C_y by a factor of about 1.5. The approximation inherent in the neglect of $C_z^2 (z_1-z_2)^2$ is slightly conservative from a structural engineering point of view (though insignificantly so). Noting, then, that for any arbitrary function, ϕ,

$$\int_0^1 \int_0^1 \phi(|Y_1-Y_2|)\, dY_1 dY_2 = \int_0^1 \phi(t)\,(1-t)\, dt \qquad (26)$$

(figure 4), and assuming $C_p(y_i,z_i) \simeq C_a$, $\overline{u(z_i)} \simeq \overline{u(z_a)}$, and $S_{u_i}(n) \simeq S_u(z_a,n)$, (i=1, 2), it follows after some algebra from equations 20, 16, and 21 that

$$S_{u,eq}(n) \simeq S_u(z_a,n)\, J(n) \qquad (27)$$

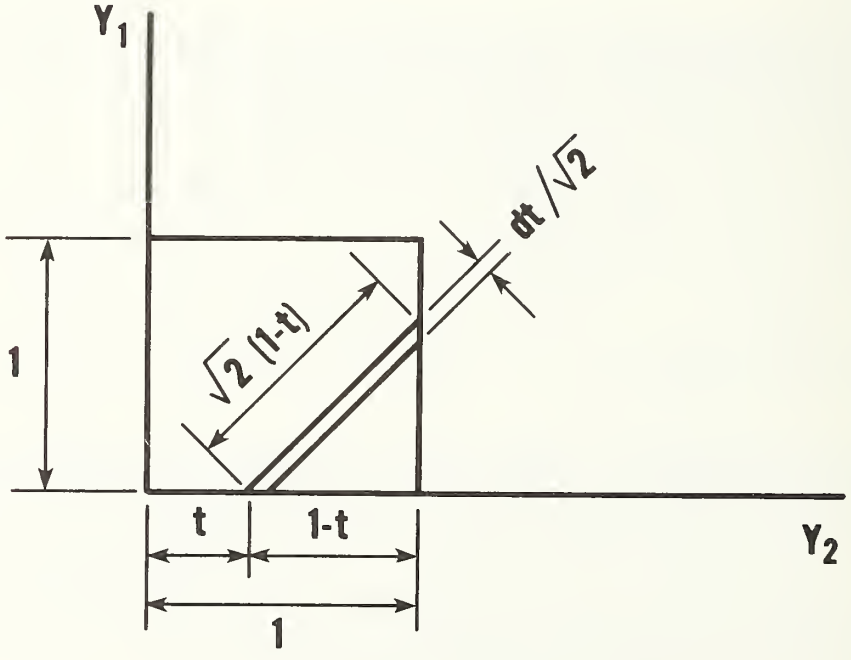

Figure 4. Integration domain and transformation of variables

where $S_u(z_a,n)$ = spectrum of longitudinal velocity fluctuations at elevation z_a given by equations A1, and $J(n)$ = reduction factor accounting for the imperfect coherence among the fluctuating wind pressures at different points of the platform, given by the expression

$$J(n) = -\frac{2}{E}\left\{-\exp(-E) + (1-\frac{1}{E})[\exp(-E)-1]\right\} \tag{28}$$

$$E = C_y\, b\, \frac{n}{\overline{u(z_a)}} \tag{29}$$

In equation 29 b = width of main deck. Equation 27 can be used in lieu of equations 20 and 21 for the Monte Carlo simulation of the equivalent velocity fluctuations $u'_{eq}(t)$ (see equation 22) needed in the expression for the total wind load acting on the platform, $F_u(t)$.

3. HYDRODYNAMIC LOADS

The total hydrodynamic load, F_h, is written in the form:

$$F_h = F_v + F_e - A\ddot{x} - B\dot{x} \tag{30}$$

where F_v = total hydrodynamic viscous force, F_e = total wave-induced exciting force, A = surge added mass, and B = surge wave-radiation damping coefficient. Following reference 17, it is assumed for convenience that the wave motion is monochromatic, hence the absence of second-order drift forces in equation 30 [16]. It is assumed in addition that B = 0 since the radiation damping at low frequencies is negligible (17, 26).

The total wave-induced exciting force and the surge added mass can be estimated numerically on the basis of potential theory. Alternatively, these two terms may be assumed to be given by the inertia component of the Morison equation, i.e.,

$$A \simeq \rho_w \sum_{ij}\sum \forall_{ij}(C_{m_{ij}} - 1) \tag{31}$$

$$F_e \simeq \rho_w \sum_{ij}\sum \forall_{ij}\, C_{m_{ij}} \left\{\frac{\partial v_{ij}}{\partial t} + [\bar{v}_i + v_{ij} - \dot{x}]\,\frac{\partial v_{ij}}{\partial X}\right\} \tag{32}$$

[18, p. 31], where ρ_w = water density, $\forall_{ij}$ = elemental volume of submerged structure, $C_{m_{ij}}$ = surge inertia coefficient corresponding to $\forall_{ij}$, X = horizontal distance from some arbitrary origin to center of $\forall_{ij}$ along direction parallel to surge motion, $\bar{v}_i$ and v_{ij} = current velocity and horizontal particle velocity due to wave motion, respectively, at center of $\forall_{ij}$. Equations 31 and 32 may be employed if for the component being considered the ratio of diameter to wave length, $D/L \leq 0.2$ [18, p.283]. Since for $T_w \simeq 15$ sec, $L = g\,T_w^2/2\pi \simeq 350$ m [18, p. 283], where T_w = wave period, and g = acceleration of gravity, it follows that for members of typical TLP structures, for which $D < 20$ m or so, the use of equations 31 and 32 is acceptable if three-dimensional flow effects are not taken into account. The wave motion is assumed to be described by deep water linear theory, so that

$$v_{ij} = \frac{\pi H}{T_w}\, e^{-kz_i} \cos\left(k_w X_j - \frac{2\pi}{T_w}t\right) \tag{33}$$

where H = wave height, k_w = wave number given by

$$k_w = \frac{1}{g}\left(\frac{2\pi}{T_w}\right)^2 \tag{34}$$

[18, p. 157]. It is recalled that the directions of the mean wind, current, and wave propagation are assumed to coincide.

The total hydrodynamic viscous load is assumed to be given by the viscous component of Morison's equation

$$F_v = 0.5\ \rho_w \sum_{ij}\sum C_{d_{ij}}\ A_{p_{ij}} |\bar{v}_i + v_{ij} - \dot{x}|[\bar{v}_i + v_{ij} - \dot{x}] \tag{35}$$

where $A_{p_{ij}}$ = area of elemental volume $\forall_{ij}$ projected on a plane normal to the direction of the current, and $C_{d_{ij}}$ = drag coefficient corresponding to $A_{p_{ij}}$.

If the relative motion of the body with respect to the fluid is harmonic, the drag and inertia coefficients in Morison's equation can be determined on the basis of experimental results as functions of local oscillatory Reynolds number, $Re = 2\pi D^2/(\nu T_f)$, Keulegan-Carpenter number, $K = \bar{V}\ T_f/D$, and relative body surface roughness, where D = diameter of body, ν = kinematic viscosity, $\bar{V}$ and T_f = amplitude and period of relative fluid-body velocity. However, actual relative fluid-body motions are not harmonic. This introduces uncertainties in the determination of the drag and inertia coefficients even if experimental information for harmonic relative motions were available in terms of Re and K. Unfortunately, such information is not available for the small K numbers (of the order of 2) and large Reynolds numbers (of the order of 10^6) of interest in TLP design. For this reason calculations will be carried out for various sets of values C_d, C_m, and the sensitivity of the results to changes in these values will be investigated.

4. RESTORING FORCE

The restoring force, R, at any instant, t, is equal to the horizontal projection of the resultant of the tether tensions at that instant, i.e.,

$$R(t) \simeq - (T+ \Delta T) \frac{x}{\ell_n + \Delta\ell_n} \tag{36}$$

where T = initial pretensioning force, ΔT = incremental tension due to surge motion, ℓ_n = nominal length of tethers at x = 0 $\Delta\ell_n$ = incremental length, and

$$\frac{T + \Delta T}{\ell_n + \Delta\ell_n} \simeq \frac{T}{\ell_n} + C_{NL} \left[1 - \sqrt{1-(x/\ell)^2}\right] \tag{37}$$

where C_{NL} = downdraw coefficient, equal to the weight of water displaced as the draft is increased by a unit length [17].

5. NUMERICAL ESTIMATES

5.1 EQUATION OF SURGE MOTION

Numerical estimates of surge motion are obtained by solving the equation of surge motion for structures with specified characteristics in specified wind, current, and wave environments. The equation of surge motion can be written as:

$$(M + A)\ddot{x} + \left[\frac{T}{\ell_n} + C_{NL}\left(1 - \sqrt{1-(x/\ell)^2}\right)\right] x =$$

$$\underbrace{0.5\ \rho_w \sum_{ij}\sum C_{d_{ij}} A_{p_{ij}} \left|\overline{v_i} + v_{ij} - \dot{x}\right| \left[v_i + v_{ij} - \dot{x}\right]}_{\text{viscous hydrodynamic force, } F_v(t) \text{ [equation 35]}}$$

$$+ \underbrace{\rho_w \sum_{ij}\sum \forall_{ij} C_{m_{ij}} \left\{\frac{\partial v_{ij}}{\partial t} + \left[\overline{v_i} + v_{ij} - \dot{x}\right] \frac{\partial v_i}{\partial X}\right\}}_{\text{wave-induced exciting force, } F_e(t) \text{ [equation 32]}}$$

$$+ \underbrace{0.5\ \rho_a\ C_a\ A_a \left[\overline{u(z_a)} + \sum_k u'_{eq,k} \cos(2\pi n_k t + \phi_k) - \dot{x}(t)\right]^2}_{\text{wind force, } F_u(t) \text{ [equations 25 and 22]}} \qquad (38)$$

The equation of motion is solved by using the PORT Ordinary Differential Equations Solution Subroutine [4]. For details on computational aspects of differential equation solutions, see references 20 and 21.

5.2 ASSUMED CHARACTERISTICS OF ENVIRONMENT AND OF PLATFORMS

The assumed characteristics of the environment and of the platforms are listed below.

(a) The current speed, v_i, varies linearly between the values given in table 1.

Table 1. Assumed Current Speeds at Various Depths z_i

z_i (meters)	$\overline{v_i}$ (meters/second)
0	1.40
35	0.90
300	0.30
550	0.15

(b) The horizontal velocities, v_{ij}, associated with the wave motion, are given by equation 33 in which H = 25 m and T_w = 15 sec.

(c) The mean wind speed is specified as $\overline{u(z_a)}$ = 45 m/s, unless otherwise stated.

(d) The equivalent wind speed fluctuation components, u'_{eqk}, are obtained by Monte Carlo simulation from the spectrum $S_{u,eq}(n)$, given by equation 27, unless otherwise stated. In equation 27, the spectrum of the longitudinal velocity fluctuations, $S_u(n)$, is given by equation A1 and A2, where the friction velocity, u_*, is obtained from equations 9 and 5, and where, unless otherwise stated, it is assumed C_{Dsea} = 0.002, L_u = 180 m, β = 6.0 (equation 14), f_m = 0.07, and f_s = 0.2. The experimental decay coefficient in the function J(n) of equation 27 (see also equations 28 and 29) is C_y = 16. However, values of C_{Dsea}, L_u, β, f_m, f_s, and C_y different from those just listed are considered in subsequent sensitivity studies.

(e) Geometric characteristics of the platforms are shown in figure 5. Unless otherwise stated, the nominal length of the tethers is assumed to be ℓ_n = 590 m, corresponding to about 600 m depth of water. The case ℓ_n = 150 m is also considered where noted.

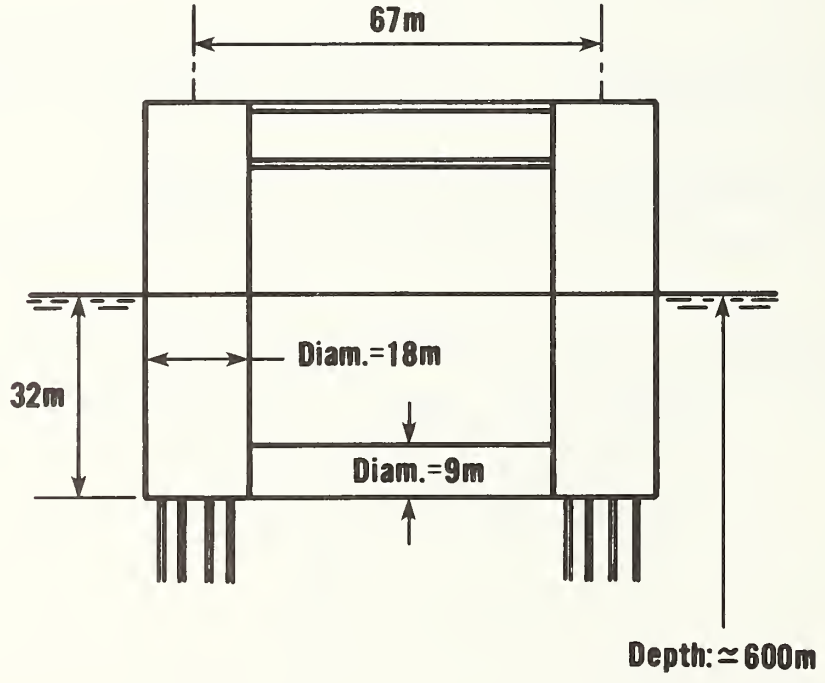

Figure 5. Geometry of tension leg platform

(f) Mechanical characteristics of the platforms are specified as follows: mass of platform, $M = 34.3 \times 10^6$ kg, total tension in legs, $T = 1.56 \times 10^5$ kN. From figure 5 it follows that $C_{NL} = 4(\pi D_c^2/4)\ \rho_w = 1.03 \times 10^4$ kN/m, where D_c = diameter of buoyant columns. Note that the values of M and T and the geometric characteristics of the platform shown in figure 5 are similar to those assumed in reference 17. This choice was aimed at facilitating comparisons with results obtained therein. Damping due to internal friction within the structure is assumed to be negligible.

(g) Hydrodynamic characteristics of the structure consist of the Morison equation coefficients. Unless otherwise stated, these are specified as $C_m = 1.8$, $C_d = 0.6$. (Note that $C_m = 1.8$ yields the surge added mass, A, obtained from calculations based on potential theory in reference 17.) In addition, the sets (a) $C_m = 1.9$, $C_d = 0.1$, (b) $C_m = 1.9$, $C_d = 0.2$, (c) $C_m = 1.8$, $C_d = 0.8$, and (d) $C_m = 1.3$, $C_d = 1.2$ (assumed to correspond to the case of submerged surfaces roughened by biofouling) are considered in sensitivity studies. Note that low C_d values have been suggested for small K numbers in low Reynolds number flow [26]. Corresponding values in the high Reynolds number regime do not appear to be available in the literature.

The nominal natural period of the surge motion, in seconds, is given by

$$T_n = 2\pi \left[\frac{(M + A)\ \ell_n}{T}\right]^{1/2} \tag{39}$$

where ℓ_n = nominal length of tethers. For the platforms with $\ell_n = 590$ m and $\ell_n = 150$ m, if $C_m = 1.8$, $T_n = 103$ sec (as in reference 17) and $T_n = 52$ sec, respectively.

(h) Aerodynamic characteristics of the structure consist of the product $0.5\ \rho_a\ C_a A_a$ (equations 17 and 19), and the elevation of the aerodynamic center, z_a. The values specified for these parameters are $0.5\ \rho_a\ C_a\ A_a = 2{,}700$ kg/m, as in reference 17, and $z_a = 50$ m. In addition, the value $z_a = 35$ m is used to investigate the influence of z_a upon the calculated surge.

5.3 LINEAR VS. NONLINEAR RESTORING FORCE

To assess the effect of neglecting the nonlinearity of the restoring force, solutions of equation 38 were obtained in which, all other parameters being the same, the cases $C_{NL} = 1.03 \times 10^4$ kN/m and $C_{NL} = 0$ were considered. In both cases it was assumed that $u'_{eq}(t)$ (see equation 22) is given by the harmonic function

$$u'_{eq}(t) = 5.9 \cos \frac{2\pi}{T_n} t \tag{40}$$

in meters per second, where $T_n = 103$ sec. It is seen from figures 6 and 7 that if the restoring force is assumed to be linear i.e., if it is assumed $C_{NL} = 0$, the surge response is amplified with respect to the nonlinear case by about 7

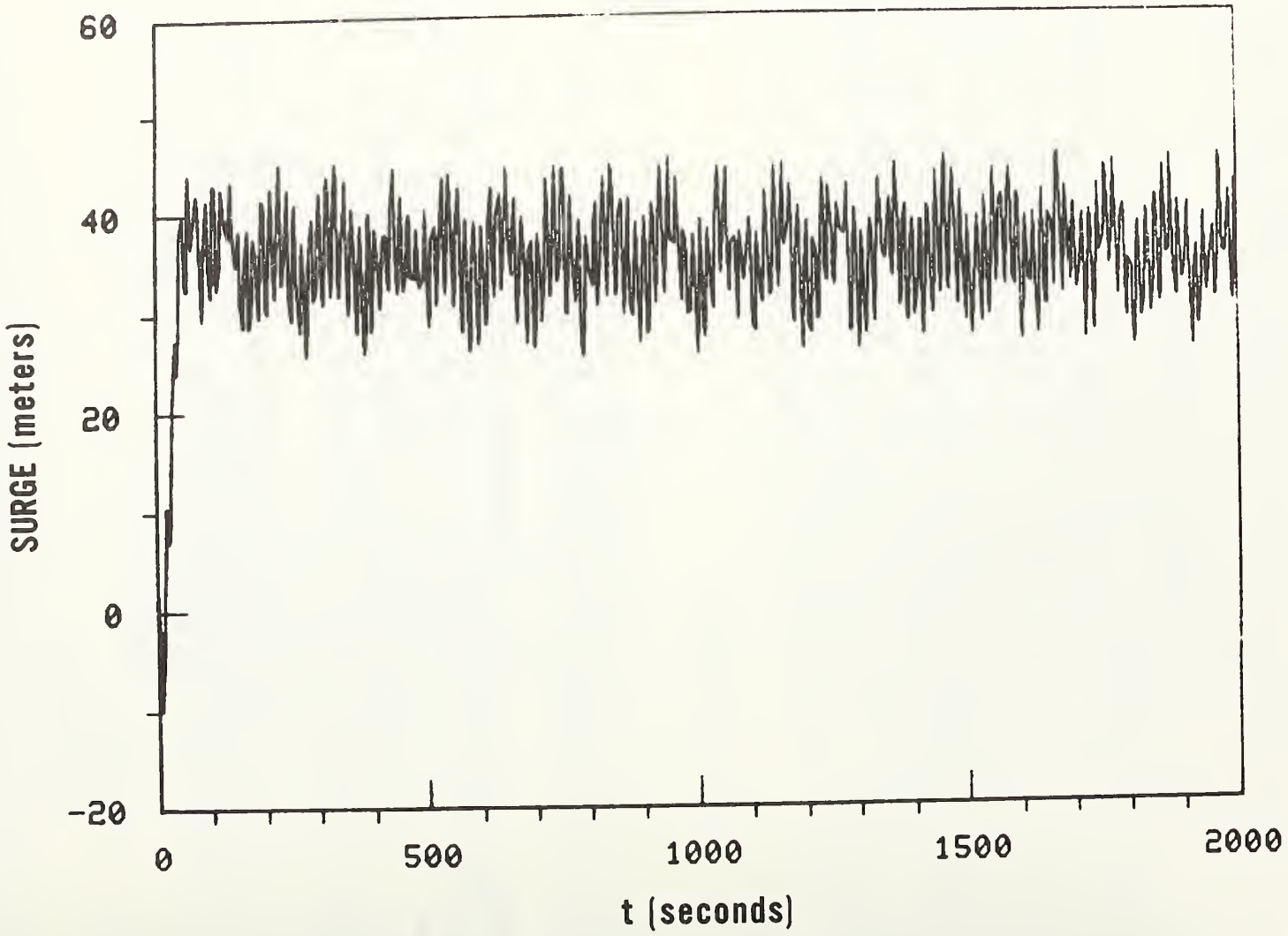

Figure 6. Surge response of tension leg platform with nonlinear restoring force

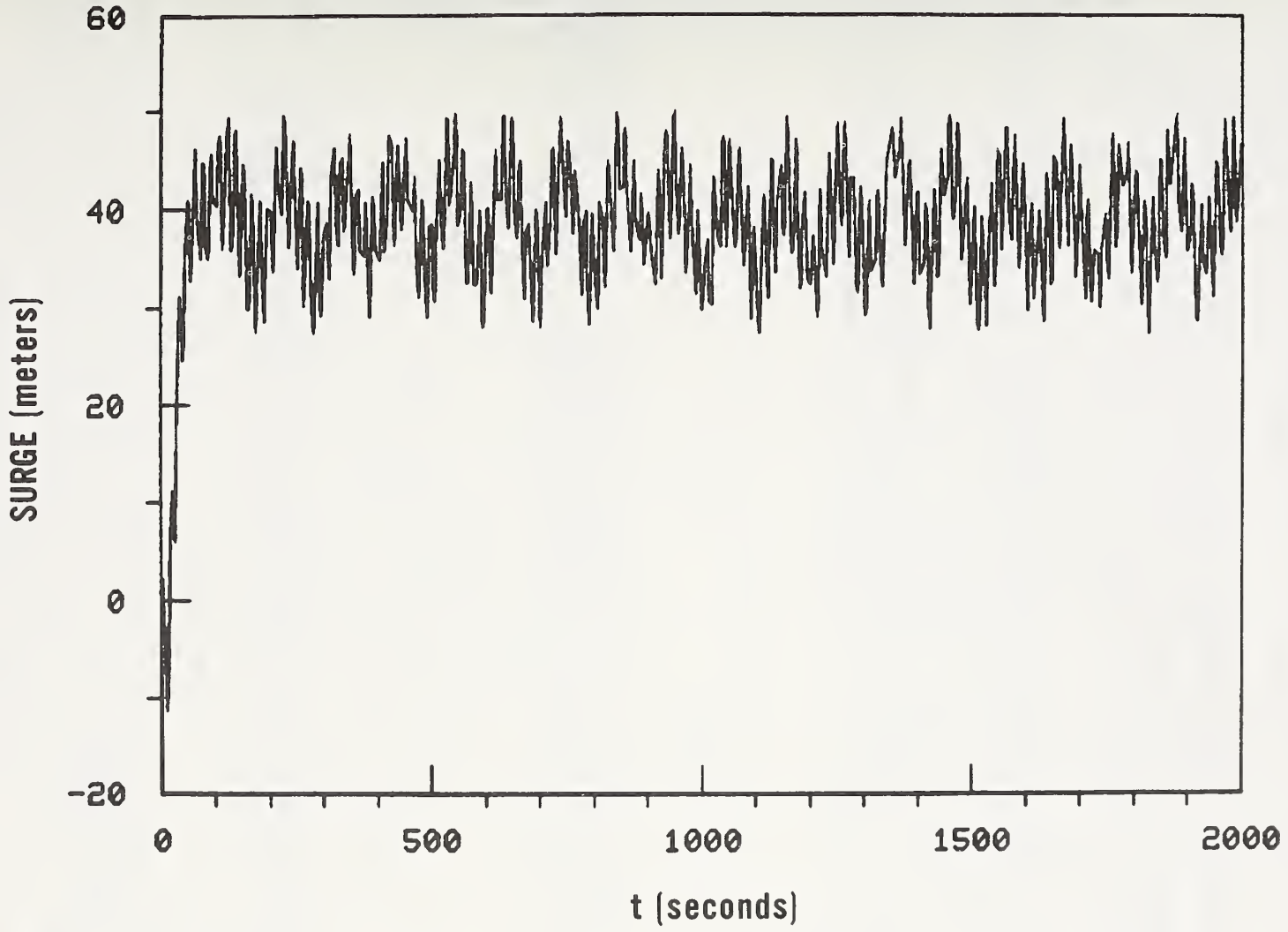

Figure 7. Surge response of tension leg platform with linear restoring force

percent. This is comparable with results reported in reference 17. Once the approximate magnitude of these differences was established, all estimates of the surge response reported in reference 17 were based on the assumption that the restoring force is linear. To facilitate comparisons with the results of reference 17, the same assumption is used henceforth in the present work.

5.4 NOMINAL DAMPING RATIO OF PSEUDO-LINEAR SYSTEM EQUIVALENT TO EQUATION 38

It was indicated previously that the estimation of the effect of turbulent wind on surge was attempted in the literature on the basis of the assumption that the equation of surge motion represents a linear system with a viscous damping term characterized by a nominal damping ratio, ζ. The effect of this term is postulated to be equivalent to the damping effect of the hydrodynamic viscous force. This approach was used, for instance, in references 6 and 28, where calculations are presented based on the assumption that ζ is of the order of 5 percent.

Such an approach is acceptable if the order of magnitude of the nominal damping ratio is consistent with the hydrodynamic behavior of the system. Calculations are now presented that illustrate how such nominal damping ratios can be estimated.

It is assumed that $u'_{eq}(t)$ (see equation 22) is given by the harmonic function

$$u'_{eq}(t) = u'_{eq1} \cos \frac{2\pi}{T_n} t \tag{41}$$

where T_n = natural period in surge, and that the system under consideration is linear with mass M + A, natural period T_n, and damping ratio ζ. The amplitude of the contribution to the surge response of a harmonic force $\rho_a C_a A_a \overline{u(z_a)} u'_{eq1} \cos 2\pi nt$ is denoted by x_{umax}, and is given by the relation:

$$x_{umax} = \frac{\rho_a C_a A_a u(z_a) u'_{eq1}}{(M+A)\left(\frac{2\pi}{T_n}\right)^2 \left\{\left[1-(nT_n)^2\right]^2 + (2\zeta nT_n)^2\right\}^{1/2}} \tag{42}$$

The nominal damping ratio, ζ, is estimated from equation 42 by equating x_{umax} and the contribution to the surge response of the force $\rho_a C_a A_a u(z_a) u'_{equ1} \cos \frac{2\pi}{T_n} t$ as obtained by solving equation 38. By substituting $1/T_n$ for n in equation 42, it follows that

$$\zeta = \frac{\frac{1}{2} \rho_a C_a A_a u(z_a) u'_{eq1}}{x_{umax} (M+A) \left(\frac{2\pi}{T_n}\right)^2} \tag{43}$$

Calculated values of ζ are shown in table 2 for the platform described previously with nominal tether lengths ℓ_n = 590 m and 150 m. These values are

based on the assumption $u(z_a) = 40$ m/s, $u'_{eql} = 4$ m/s. For example, in the case $\ell_n = 590$ m, $C_m = 1.8$, $C_d = 0.8$, equation 38 yields $x_{umax} \simeq 2.5$ m (i.e., half the double amplitude of the low frequency oscillation in figure 8). Since M+A = 71.1 x 10^6 kg, $T_n = 103$ sec, and $0.5\ \rho_a\ C_a\ A_a = 2{,}700$ kg/m, the estimated nominal damping ratio in this case is $\zeta = 0.65$. Results are given in table 2 for each of the five sets of values C_m, C_d listed previously. Also shown in table 2 are calculated values of the steady and peak surge response in meters. It is seen that as the damping coefficient, C_d, increases, both the steady and the peak response increase, even though the contribution to the response due to wind speed fluctuations decreases as a result of the stronger hydrodynamic damping.

It is seen in table 2 that the estimated damping ratios are considerably larger than assumed, e.g., in references 6 and 28. Large values of ζ indicate that the damping inherent in the viscous hydrodynamic forces is sufficiently strong to preclude the occurrence of significant resonant amplification effects under fluctuating wind loads. Note that results similar to those of table 2 are obtained from the surge response calculations reported in reference 17.

Table 2. Estimated Nominal Damping Ratio, ζ, and Mean and Peak Surge Response $\bar{x}$ and x_{pk}, in Meters

		ℓ_n = 590 meters			ℓ_n = 150 meters		
C_m	C_d	ζ	$\bar{x}$ meters	x_{pk} meters	ζ	$\bar{x}$ meters	x_{pk} meters
1.9	0.1	0.25	25.	36.0	0.10	6.0	15.5
1.9	0.2	0.30	28.5	38.0	0.15	7.0	16.0
1.8	0.6	0.55	34.	43.0	0.20	9.0	17.0
1.8	0.8	0.65	37.	44.5	0.30	10.0	18.0
1.3	1.2	0.80	46.	56.0	N.C.[a]	N.C.[a]	N.C.[a]

[a] N.C. = not calculated

The results of table 2 suggest that, unless biofouling effects are significant, it is reasonable to assume for the purpose of estimating peak surge response that $C_d = 0.6$, $C_m = 1.8$. This set of values is used subsequently in this paper for the estimation of surge response under turbulent wind loads.

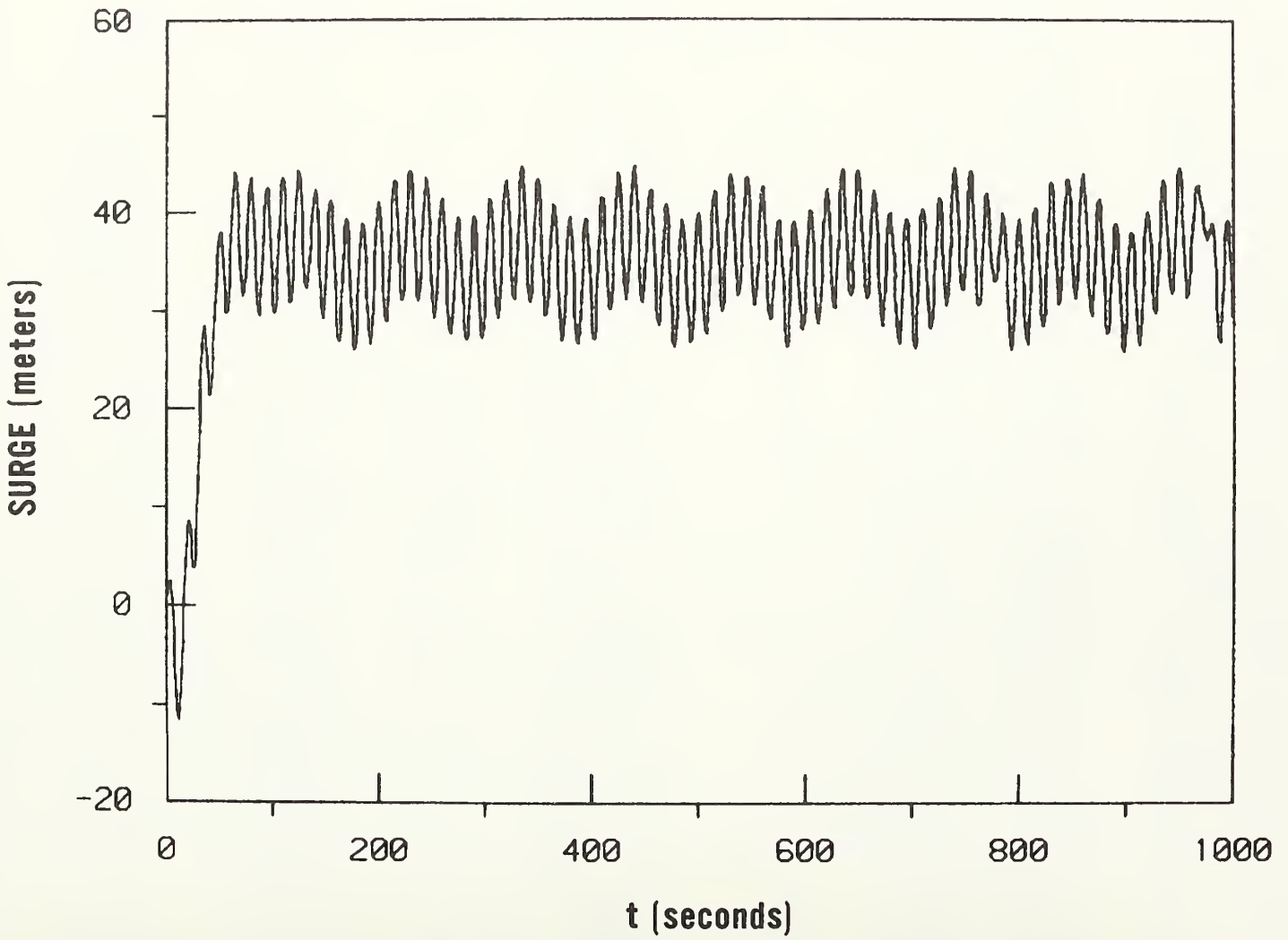

Figure 8. Surge response of tension leg platform to harmonic wind load in the presence of current and waves, $C_m = 1.8$, $C_d = 0.8$

5.5 PEAK SURGE RESPONSE UNDER TURBULENT WINDS

The equation of surge motion (equation 38), with the environmental, geometric, mechanical, hydrodynamic, and aerodynamic parameters specified previously, was solved for fifty different realizations of the random process $u'_{eq}(t)$ (equation 22) in each of the following cases: ℓ_n = 590 m and ℓ_n = 150 m. The sample mean, $\overline{x_{max}}$, the sample standard deviation, $s(x_{max})$, and the sample maximum $Max(x_{max})$, of the peak surge response, x_{max}, are listed in line (1) of table 3 (corresponding to L_u = 180 m). A typical solution of equation 38 is shown in figure 9 for the platform with ℓ_n = 590 m (T_n = 103 sec), and L_u = 180 m.

Table 3. Statistics of Peak Surge Response, x_{max}, Under Turbulent Winds (in meters)

	ℓ_n = 590 m (T_n = 103 sec)			ℓ_n = 150 m (T_n = 52 sec)		
	$\overline{x_{max}}$	$s(x_{max})$	$Max(x_{max})$	$\overline{x_{max}}$	$s(x_{max})$	$Max(x_{max})$
(1) L_u = 180 m	48.7	1.19	51.4	18.3	0.40	19.7
(2) L_u = 100 m	48.1	0.64	49.9	18.2	0.44	19.5
(3) L_u = 240 m	48.9	1.13	51.7	18.5	0.50	19.8

5.6 SURGE RESPONSE ESTIMATED UNDER VARIOUS SIMPLIFYING ASSUMPTIONS

It is of interest to estimate the surge response that would occur if the platform were subjected to forces induced by:

Case A: Mean wind alone
Case B: Current and waves alone
Case C: Current, waves, and mean wind alone (no wind speed fluctuations)
Case D: Current, waves, mean wind, and harmonic wind speed fluctuations $u_{eq}(t) = 0.1\, u(z_a) \cos(2\pi t/T_n)$
Case E: Current, waves, mean wind, and harmonic wind speed fluctuations, $u_{eq}(t) = 1.41\sqrt{\beta u_*}\cos 2\pi\, t/T_n)$ [recall that $\sqrt{\beta u_*}$ = r.m.s. of turbulent wind speed fluctuations - see equation 14].
Case F: Current, waves, and steady (1-minute) wind speed [No wind speed fluctuations]. (Note that 1-minute speed $\simeq 1.24\, u(z_a)$, see reference 23, p. 62.)

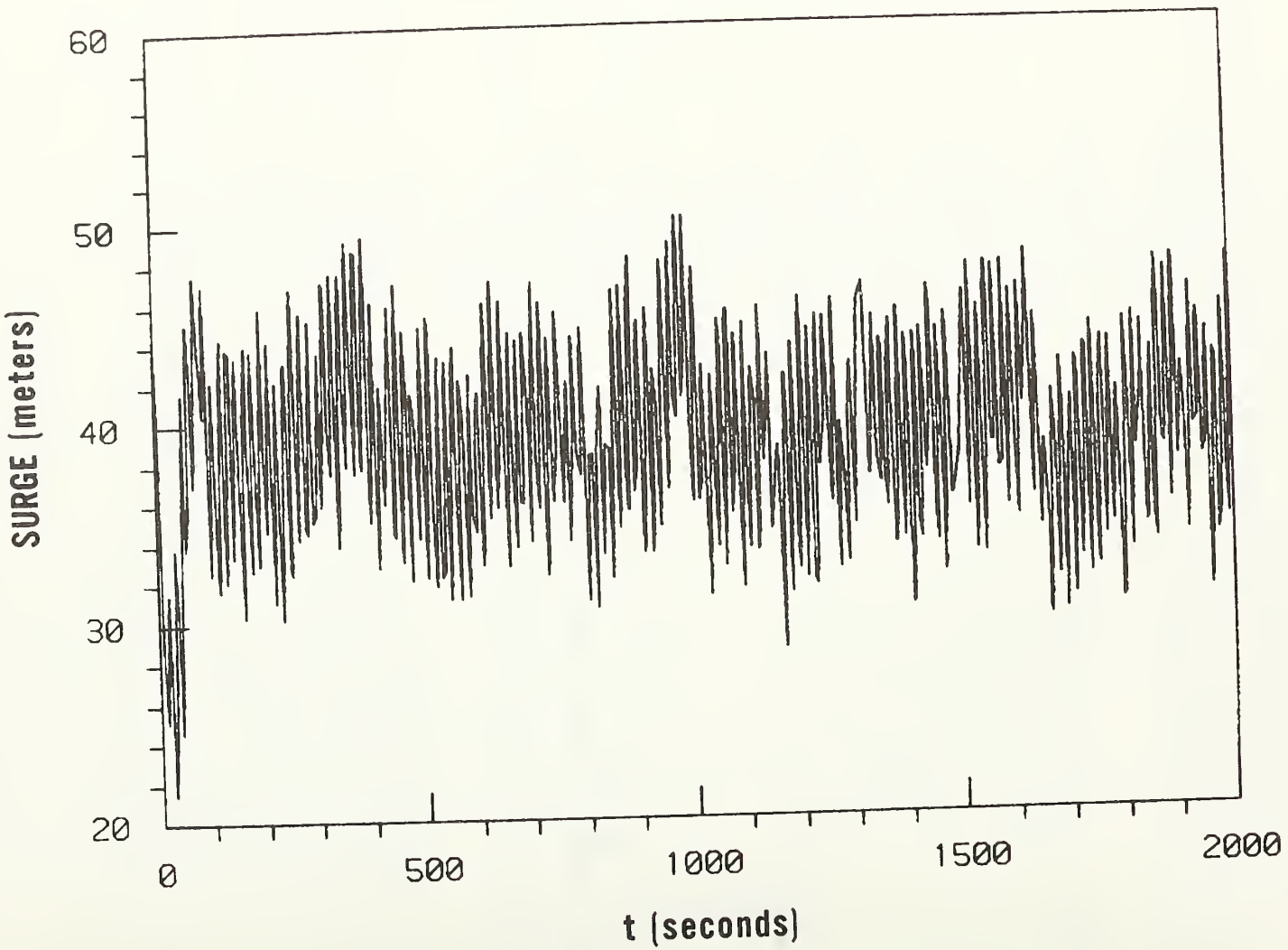

Figure 9. Surge response of tension leg platform to turbulent wind load in the presence of current and waves

The results of the calculations are shown in table 4, which lists for each of these cases the peak surge, as well as the steady surge, the amplitude of the wave-induced fluctuating surge, and the amplitude of the wind-induced fluctuating surge.

The results of tables 3 and 4 show that:

- The contribution of the mean wind to the peak surge response is about 40 percent and 25 percent for the platforms with ℓ_n = 590 m, and ℓ_n = 150 m, respectively (case A, table 4, versus Max(m_{max}), line (1), table 3).

- The contribution of the wind speed fluctuations to the peak surge response is about 12 percent for both values of ℓ_n (case C, table 4, versus Max(x_{max}), line (1), table 3).

- The contribution of current and waves to the peak surge response is about 50 percent and 60 percent for the platforms with ℓ_n = 590 m and ℓ_n = 150 m, respectively (case B, table 4, versus Max(x_{max}), table 3).

- Representing the turbulent wind speed fluctuations by a harmonic fluctuation with amplitude equal to one-tenth of the mean wind speed, as done in reference 17, (case D), results in an underestimation of peak surge response by 5 percent to 10 percent. Calculations were carried out which showed that, in order for harmonic and turbulent wind speed fluctuations to be equivalent in terms of surge response, the amplitude of the harmonic wind speed fluctuations should be about twice the r.m.s. of the turbulent wind fluctuations.

Table 4. Estimates of Surge Response Corresponding to Various Deterministic Loading Assumptions (in meters)

Case	ℓ_n = 590 m				ℓ_n = 150 m			
	Steady	Wave-Induced Fluct.	Wind-Induced Fluct.	Total (peak)	Steady	Wave-Induced Fluct.	Wind-Induced Fluct.	Total (peak)
A	20.5	-	-	20.5	5.3	-	-	5.3
B	18.0	6.5	-	24.5	4.5	7.5	-	12.0
C	39.0	6.0	-	45.0	10.0	7.5	-	17.5
D	39.0	5.0	5.0	49.0	10.0	6.0	2.0	18.0
E	39.0	5.0	5.5	49.5	10.0	6.0	2.5	18.5
F	50.0	6.0	-	56.0	13.5	6.5	-	20.0

- Accounting for the contribution of the wind speed fluctuations to the peak surge response by assuming $u'_{eq}(t) = 0$ and replacing $\overline{u(z_a)}$ in equation 25 by the one-minute wind speed, as done in references 11 and 18 (case F), results in an overestimation of the total peak surge by about 10 percent for the platform with $\ell_n = 590$ m, and 1 percent for the platform with $\ell_n = 150$ m.

5.7 SENSITIVITY OF SURGE RESPONSE TO CHANGES IN VALUES OF WIND ENVIRONMENT AND AERODYNAMIC PARAMETERS

This section examines the effect upon the surge response of changes in the values of the wind environment parameters L_u, f_m, f_s, C_z and C_y, and C_{Dsea} (or z_o - see equation 5), and of the aerodynamic parameter z_a.

The effect of the magnitude of the integral turbulence scale, L_u, is investigated by estimating the surge response under the same assumptions that led to the results of line (1) of table 3, except that in lieu of $L_u = 180$ m the values $L_u = 100$ m and $L_u = 240$ m are used. Again, for each of the cases $\ell_n = 590$ and $\ell_n = 150$ m, equation 38 was solved for fifty different realizations of the random process $u'_{eq}(t)$. The results are given in lines (2) and (3) of table 3. It is seen that the statistics of the peak response are not affected significantly by L_u; the sample maxima, $\text{Max}(x_{max})$, differ in both cases by 3.5 percent or less when the integral scale of turbulence increases by a factor of 2.4.

An inspection of figure 2 and 3 shows that the influence upon the spectral shape of the nondimensional frequency, f_m, at which $nS_u(n)$ is maximum (see equation A1), is considerably weaker than the influence of L_u. Hence, it can be expected that the influence of f_m on the surge response is minimal. Solutions of equation 38 in which the values $f_m = 0.04$ and $f_m = 0.10$, in lieu of $f_m = 0.07$, were used, all other parameters being unchanged, showed that this is indeed the case.

The nondimensional frequency f_s (see equation A1) affects the higher frequency portion of the spectrum, which has no perceptible influence on the surge response. Hence, even large variations of f_s (between 0.1 and 1, say) are inconsequential as far as their effect on surge is concerned.

It is well known that the average size of the longitudinal turbulent eddies in the atmosphere is considerably less in the transverse than in the longitudinal direction [22, 23]. For this reason $C_z < C_y$, the ratio C_z/C_y being about 0.6 or less. It was pointed out previously that for typical platform shapes this results in the effect of C_z being negligible with respect to the effect of C_y in equation 16 and 20, so that equation 27 through 29 may be used in lieu of equation 21. If the value $C_y = 24$ in lieu of $C_y = 16$ is used, the values of $J^{1/2}(n)$ in and near the range of frequencies where the energy of the wind speed fluctuations is large ($0 < n < 0.5$ or so - see figure 2) decrease as shown in table 5.

Table 5. Dependence of $J^{1/2}(n)$ Upon Exponential Decay Coefficient, C_y

n	0.01	0.02	0.05	0.1
$J^{1/2}$ (C_y = 16, n)	0.95	0.91	0.79	0.68
$J^{1/2}$ (C_y = 24, n)	0.93	0.87	0.73	0.59

It is seen that the influence of large changes in the value of C_y upon $J^{1/2}(n)$ in this frequency range is on the average of a few percent. It follows that the influence of such changes on the peak surge response is negligible for practical purposes.

The choice of value C_{Dsea} affects both the mean wind profile and the spectrum of the longitudinal velocity fluctuations. To C_{Dsea} = 0.002 and 0.003, for example, there correspond values z_o = 0.0013 m and 0.0067 m, respectively (equation 5). Based on equation 4, the respective calculated mean speeds at z = 20 m and z = 50 m above mean water level, given that $\overline{u(35\ m)}$ = 45 m/s, are listed in table 6.

Table 6. Dependence of $\overline{u(z)}$ Upon z_o ($\overline{u(35m)}$ = 45 m/s)

Elevation, z	20 m	50 m
$\overline{u(z)}$ for z_o = 0.0013 m	42.4 m/s	46.5 m/s
$\overline{u(z)}$ for z_o = 0.0067 m	42.0 m/s	46.8 m/s

The influence of C_{Dsea} is more significant in the case of the spectra, $S_u(n)$, which are proportional to u_*^2 (equations A1). To differences between values of C_{Dsea} of the order of 50 percent there correspond differences in the magnitude of $S_u^{1/2}(n)$ of about 20 percent. Owing to nonlinearity effects, the differences between the corresponding contributions of the wind speed fluctuations to the surge response are somewhat less. Since these contributions were previously estimated to be of about 12 percent of the peak surge response, differences between C_{Dsea} values of the order of 50 percent result in differences between the corresponding values of the peak surge response of less than 3 percent.

To summarize, although the uncertainties with respect to the parameters defining the wind environmental are large, the effects of these uncertainties upon the peak response translate in all cases into differences of the order of a few percent.

The aerodynamic parameter z_a used in the calculations presented so far was specified as $z_a = 50$ m, as indicated previously. Lower values, e.g. $z_a = 35$ m, may be encountered in typical practical situations. Calculations based on the assumption $z_a = 35$ m, all other parameters being unchanged (including the speed $\overline{u(z_a)} = 45$ m/s), have shown that the peak surge response is smaller by less than 2 percent than the corresponding response based on the value $z_a = 50$ m.

6. SUMMARY AND CONCLUSIONS

This paper presents a procedure for estimating surge response to the action of turbulent winds in the presence of current and waves. The procedure accounts for the nonlinearity of the hydrodynamic forces and the coupling of aerodynamic and hydrodynamic effects.

It is demonstrated that, unlike wave spectra, wind spectra peak at zero frequency, where they are proportional to the integral scale of turbulence. An expression for the wind spectrum consistent with this requirement is derived, and a critique is presented of current expressions in which this requirement is violated. It is shown that such expressions may lead to the gross underestimation of wind speed fluctuation components with frequencies comparable to the natural frequencies of compliant platforms.

A simple expression is derived that accounts for the imperfect coherence of fluctuating wind pressures acting at different points on the surface of the platform.

For illustrative purposes the procedure for estimating surge response is applied to typical tension leg platforms (TLP's) for water depths of about 600 m and 150 m. Solutions of the equation of surge motion are obtained, which suggest that for these platforms the hydrodynamic damping is sufficiently large to preclude the occurrence of significant resonant amplification effects due to wind loads, even if the assumed drag coefficients in Morison's equation are as low as $C_d = 0.1$. Equivalent linear damping ratios with respect to wind effects were estimated to be of the order of 25 percent to 55 percent corresponding to $C_d = 0.1$ and $C_d = 0.6$, respectively, in 600 m deep waters, and 10 percent to 20 percent for $C_d = 0.1$ and $C_d = 0.6$, respectively, in 150 m deep waters. The calculations show that as the viscous damping due to hydrodynamic effects increases, the peak total surge response also increases, even though the contribution of the fluctuating wind effects to the total surge is reduced. The use of a Morison equation drag coefficient $C_d = 0.6$ appears to be reasonable for the purpose of estimating peak total surge.

Parameters defining the wind environment are reviewed, and it is shown that uncertainties with respect to the actual values of these parameters have little effect on the estimated peak surge response. However, uncertainties with respect to the sea surface drag coefficient (or equivalently, to the roughness length parameter for the sea surface) may cause differences of the order of 20 percent in the estimated contribution of the wind load fluctuations to the surge response.

For the platforms considered in this work, and under the assumption that the drag coefficient in Morison's equation is $C_d = 0.6$, a fictitious harmonic wind speed fluctuation and the actual turbulent wind speed fluctuations are equivalent from the standpoint of their contribution to the total surge if the amplitude of the harmonic fluctuations is equal to about twice the r.m.s. of the turbulent fluctuations. Finally, it is concluded that, under the same assumption, the use of a one-minute wind speed to represent the effect of the mean wind and of the turbulent wind fluctuations is acceptable for the purpose of estimating peak surge response.

REFERENCES

1. American National Standard Building Code Requirements for Minimum Design Loads in Buildings and Other Design Loads in Buildings and Other Structures, A58.1, American National Standards Institute, New York, 1972.

2. Counihan, J., "Adiabatic Atmospheric Boundary Layers: A Review and Analysis of Data from the Period 1880-1972," Atmospheric Environment, Vol. 9, (1975), pp. 871-905.

3. Davenport, A.G., "The Dependence of Wind Load Upon Meteorological Parameters," Proceedings, International Research Seminar on Buildings and Structures, University of Toronto Press, Toronto, 1968, pp. 19-82.

4. Fox, P.A., ed., PORT Mathematical Subroutine Library, Bell Laboratories Computing Information Service, 600 Mountain Avenue, Murray Hill, N.J., 1976.

5. Garratt, J.R., "Review of Drag Coefficients over Oceans and Continents," Monthly Weather Review, Vol. 105, July 1977, pp. 915-929.

6. Kareem, A. and Dalton, C., "Dynamic Effects of Wind on Tension Leg Platforms," OTC 4229, Proceedings, 14th Annual Offshore Technology Conference, Vol. 1, pp. 749-757, Houston, TX, May 1982.

7. Kristensen, L., "On Longitudinal Spectral Coherence," Boundary-Layer Meteorology, Vol. 16 (1979), pp. 145-153.

8. Kristensen, L. and Jensen, N.O., "Lateral Coherence in Isotropic Turbulence and in the National Wind," Boundary-Layer Meteorology, Vol. 17 (1979), pp. 353-373.

9. Krügermeyer, L., Grünewald, M., and Dunckel, M., "The Influence of Sea Waves on the Wind Profile," Boundary-Layer Meteorology, Vol. 14 (1978), pp. 403-414.

10. Lumley, J.L. and Panofsky, H.A., The Structure of Atmospheric Turbulence, Wiley, New York, 1964.

11. Mercier, J.A., Leverette, S.J., and Bliault, A.L., "Evaluation of Hutton TLP Response to Environmental Loads," OTC 4429, Proceedings, 14th Annual Offshore Technology Conference, Vol. 4, Houston, Tx, May, 1982, pp. 585-602.

12. National Building Code of Canada, Commentaries on Part 4, Supplement No. 4, NRCC No.13989, Canadian Structural Design Manual, Associate Committee on the National Building Code and National Research Council of Canada, Ottawa, 1975.

13. Owen, P.R., "Buildings in the Wind," Quarterly Journal of the Royal Meteorological Society, Vol. 97 (1978), pp. 396-413.

14. Panofsky, H.A., et al., "Two-Point Velocity Statistics over Lake Ontario," Boundary Layer Meteorology, Vol. 7 (1974), pp. 309-321.

15. Pasquill, F. and Butler, H.E., "A Note on Determining the Scale of Turbulence," Quarterly Journal of the Royal Meteorological Society, Vol. 90 (1964), pp. 79-84.

16. Pinkster, J.A. and Van Oortmerssen, G., "Computation of First- and Second-Order Forces on Oscillating Bodies in Regular Waves, Proceedings, Second International Conference on Ship Hydrodynamics, U.C. Berkeley, Cal., 1977.

17. Salvesen, N., et al., "Computations of Nonlinear Surge Motions of Tension Leg Platforms," OTC 4394, Proceedings, Offshore Technology Conference, Vol. 4, Houston, TX, May 1982, pp. 199-216.

18. Sarpkaya, T. and Isaacson, M., Mechanics of Wave Forces on Offshore Structures, Van Nostrand Reinhold Co., New York, 1981.

19. Sebastiani, G., Della Greca, A., and Bucaneve, G., "Characteristics and Dynamic Behavior of Tecnomare's Tension Leg Platform," in Hydrodynamics in Ocean Engineering, The Norwegian Institute of Technology, Trondheim, August 1981, pp. 947-962.

20. Shampine, I.F., What Everyone Solving Differential Equations Should Know, Sandia Labs, Albuquerque, N.M., March 1979, NTIS Pamphlet No. SAND-78-0315.

21. Shampine, L.F., Watts, H.A., Davenport, S.M., "Solving Non-Stiff Ordinary Differential Equations - The State of the Art," SIAM Review, Vol. 18, No. 3, July 1976, pp. 376-411.

22. Shiotani, M. and Iwatani, Y., "Correlations of Wind Velocities in Relations to the Gust Loadings," Proceedings, Third International Conference on Wind Effects on Buildings and Structures, Tokyo, 1971, Saikon, Tokyo, 1972, pp. 57-67.

23. Simiu, E. and Scanlan, R.H., Wind Effects on Structures, Wiley-Interscience, New York, N.Y., 1978.

24. Smith, J.R. and Taylor, R.S., "The Development of Articulated Buoyant Column Systems as an Aid to Economic Offshore Production," EUR 226, Proceedings, European Offshore Petroleum Conference Exhibition, London, England, Oct. 1980, pp. 545-557.

25. Smith, S.D. and Banke, E.G., "Variation of the Sea Surface Drag Coefficient with Wind Speed," Quarterly Journal of the Royal Meteorological Society, Vol. 101 (1975), pp. 665-673.

26. Verley, R. and Moe., G., The Forces on a Cylinder Oscillating in a Current, SINTEF Report No. STF60 A79061, Trondheim, Norway, 1979.

27. Vickery, B.J., "On the Reliability of Gust Loading Factors," Proceedings, Technical Meeting Concerning Wind Loads on Buildings and Structures, National Bureau of Standards, Building Science Series 30, Washington, D.C., 1970, pp. 93-104.

28. Vickery, B.J., "Wind Loads on Compliant Offshore Structures," Proceedings, Ocean Structural Dynamics Symposium, Oregon State University, Dept. of Civil Engineering, Corvallis, Oregon, Sept. 1982, pp. 632-648.

29. Wu, J., "Wind Stress and Surface Roughness at Air-Water Interface," Journal of Geophysical Research, Vol. 74 (1969), pp. 444-455.

APPENDIX: EXPRESSION FOR THE SPECTRUM OF THE LONGITUDINAL VELOCITY FLUCTUATIONS

$$\frac{n\,S_u(z,n)}{u_*^2} = \begin{cases} a_1 f + b_1 f^2 + d_1 f^3 & f \le f_m \quad \text{(A1a)} \\ c_2 + a_2 f + b_2 f^2 & f_m < f < f_s \quad \text{(A1b)} \\ 0.26\, f^{-2/3} & f \ge f_s \quad \text{(A1c)} \end{cases}$$

where u_* is given by equations 9 and 4, $f = nz/\overline{u(z)}$, and

$$a_1 = \frac{4\,L_u\,\beta}{z} \quad \text{(A2a)}$$

$$\beta_1 = 0.26\, f_s^{-2/3} \quad \text{(A2b)}$$

$$b_2 = \frac{\frac{1}{3}a_1 f_m + (\frac{7}{3} + \ell n\,\frac{f_s}{f_m})\beta_1 - \beta}{\frac{5}{6}(f_m - f_s)^2 + \frac{1}{2}(f_m^2 - f_s^2) + 2f_m(f_s - f_m) + f_s(f_s - 2f_m)\ell n\frac{fs}{fm}} \quad \text{(A2c)}$$

$$a_2 = -2\,b_2\,f_m \quad \text{(A2d)}$$

$$d_1 = \frac{2}{f_m^3}\left[\frac{a_1 f_m}{2} - \beta_1 + b_2\,(f_m - f_s)^2\right] \quad \text{(A2e)}$$

$$b_1 = \frac{-a_1}{2f_m} - 1.5\,f_m d_1 \quad \text{(A2f)}$$

$$c_2 = \beta_1 - a_2 f_s - b_2 f_s^2 \quad \text{(A2g)}$$

☆ U.S. GOVERNMENT PRINTING OFFICE : 1983 O—380-997 (908)

NBS-114A (REV. 2-8C)

U.S. DEPT. OF COMM. BIBLIOGRAPHIC DATA SHEET (See instructions)	1. PUBLICATION OR REPORT NO. NBS BSS 151	2. Performing Organ. Report No.	3. Publication Date March 1983

4. TITLE AND SUBTITLE

Turbulent Wind Effects on Tension Leg Platform Surge

5. AUTHOR(S)

Emil Simiu and Stefan D. Leigh

6. PERFORMING ORGANIZATION (If joint or other than NBS, see instructions)

NATIONAL BUREAU OF STANDARDS
DEPARTMENT OF COMMERCE
WASHINGTON, D.C. 20234

7. Contract/Grant No.

8. Type of Report & Period Covered

Final

9. SPONSORING ORGANIZATION NAME AND COMPLETE ADDRESS (Street, City, State, ZIP)

Minerals Management Service
U.S. Department of the Interior
Reston, VA 22091

10. SUPPLEMENTARY NOTES

Library of Congress Catalog Card Number: 83-600507

☐ Document describes a computer program; SF-185, FIPS Software Summary, is attached.

11. ABSTRACT (A 200-word or less factual summary of most significant information. If document includes a significant bibliography or literature survey, mention it here)

A procedure is presented for estimating surge response to turbulent wind in the presence of current and waves. The procedure accounts for the nonlinearity of the hydrodynamic forces with respect to surge and for the coupling of aerodynamic and hydrodynamic effects. It is shown that current wind spectra do not model correctly the wind speed fluctuations at very low frequencies and an alternative model of the wind spectrum, consistent with fundamental principles, is presented. The equation of surge motion under turbulent wind in the presence of current and waves is solved for typical tension leg platforms, and it is shown that under extreme wave conditions the damping provided by the hydrodynamic forces precludes the occurrence of significant wind-induced resonant amplification effects even if the drag coefficient in the Morison equation is very small (e.g., $C_d = 0.1$). It is verified that for the platforms being investigated the use of a one-minute wind speed to represent the effect of the mean wind and of the turbulent wind fluctuations is acceptable for the purpose of estimating peak surge response.

12. KEY WORDS (Six to twelve entries; alphabetical order; capitalize only proper names; and separate key words by semicolons)

compliant platforms; ocean engineering; offshore platforms; structural engineering; tension leg platforms; turbulence; waves; wind loads.

13. AVAILABILITY

☒ Unlimited

☐ For Official Distribution. Do Not Release to NTIS

☒ Order From Superintendent of Documents, U.S. Government Printing Office, Washington, D.C. 20402.

☐ Order From National Technical Information Service (NTIS), Springfield, VA. 22161

14. NO. OF PRINTED PAGES

46

15. Price

$4.75

NBS TECHNICAL PUBLICATIONS

PERIODICALS

JOURNAL OF RESEARCH—The Journal of Research of the National Bureau of Standards reports NBS research and development in those disciplines of the physical and engineering sciences in which the Bureau is active. These include physics, chemistry, engineering, mathematics, and computer sciences. Papers cover a broad range of subjects, with major emphasis on measurement methodology and the basic technology underlying standardization. Also included from time to time are survey articles on topics closely related to the Bureau's technical and scientific programs. As a special service to subscribers each issue contains complete citations to all recent Bureau publications in both NBS and non-NBS media. Issued six times a year. Annual subscription: domestic $18; foreign $22.50. Single copy, $5.50 domestic; $6.90 foreign.

NONPERIODICALS

Monographs—Major contributions to the technical literature on various subjects related to the Bureau's scientific and technical activities.

Handbooks—Recommended codes of engineering and industrial practice (including safety codes) developed in cooperation with interested industries, professional organizations, and regulatory bodies.

Special Publications—Include proceedings of conferences sponsored by NBS, NBS annual reports, and other special publications appropriate to this grouping such as wall charts, pocket cards, and bibliographies.

Applied Mathematics Series—Mathematical tables, manuals, and studies of special interest to physicists, engineers, chemists, biologists, mathematicians, computer programmers, and others engaged in scientific and technical work.

National Standard Reference Data Series—Provides quantitative data on the physical and chemical properties of materials, compiled from the world's literature and critically evaluated. Developed under a worldwide program coordinated by NBS under the authority of the National Standard Data Act (Public Law 90-396).

NOTE: The principal publication outlet for the foregoing data is the Journal of Physical and Chemical Reference Data (JPCRD) published quarterly for NBS by the American Chemical Society (ACS) and the American Institute of Physics (AIP). Subscriptions, reprints, and supplements available from ACS, 1155 Sixteenth St., NW, Washington, DC 20056.

Building Science Series—Disseminates technical information developed at the Bureau on building materials, components, systems, and whole structures. The series presents research results, test methods, and performance criteria related to the structural and environmental functions and the durability and safety characteristics of building elements and systems.

Technical Notes—Studies or reports which are complete in themselves but restrictive in their treatment of a subject. Analogous to monographs but not so comprehensive in scope or definitive in treatment of the subject area. Often serve as a vehicle for final reports of work performed at NBS under the sponsorship of other government agencies.

Voluntary Product Standards—Developed under procedures published by the Department of Commerce in Part 10, Title 15, of the Code of Federal Regulations. The standards establish nationally recognized requirements for products, and provide all concerned interests with a basis for common understanding of the characteristics of the products. NBS administers this program as a supplement to the activities of the private sector standardizing organizations.

Consumer Information Series—Practical information, based on NBS research and experience, covering areas of interest to the consumer. Easily understandable language and illustrations provide useful background knowledge for shopping in today's technological marketplace.

Order the **above** *NBS publications from: Superintendent of Documents, Government Printing Office, Washington, DC 20402.*

Order the **following** *NBS publications—FIPS and NBSIR's—from the National Technical Information Service, Springfield, VA 22161.*

Federal Information Processing Standards Publications (FIPS PUB)—Publications in this series collectively constitute the Federal Information Processing Standards Register. The Register serves as the official source of information in the Federal Government regarding standards issued by NBS pursuant to the Federal Property and Administrative Services Act of 1949 as amended, Public Law 89-306 (79 Stat. 1127), and as implemented by Executive Order 11717 (38 FR 12315, dated May 11, 1973) and Part 6 of Title 15 CFR (Code of Federal Regulations).

NBS Interagency Reports (NBSIR)—A special series of interim or final reports on work performed by NBS for outside sponsors (both government and non-government). In general, initial distribution is handled by the sponsor; public distribution is by the National Technical Information Service , Springfield, VA 22161, in paper copy or microfiche form.

U.S. Department of Commerce
National Bureau of Standards

Washington, D.C. 20234
Official Business
Penalty for Private Use $300

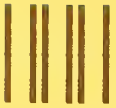

POSTAGE AND FEES PAID
U.S. DEPARTMENT OF COMMERCE
COM-215

THIRD CLASS
BULK RATE